

University of Nottingham
DEPARTMENT OF CIVIL ENGINEERING
CIVE4044

FINITE ELEMENT ANALYSIS OF RAILWAY SLAB TRACK
STRUCTURE



by

Mehmethan Oncel

September 2020

A report submitted in part consideration of the degree of MSc in Transportation
Infrastructure Engineering: Sustainable Railways

Abstract

With the increasing travel demand in the world, it is aimed to shorten travel times and to develop faster transportation preferences. One of them is high-speed train projects. Conventional infrastructure systems have begun to not respond to the increase in train speeds in railways, and innovative approaches, the leading of which were slab track designs, have been started to be developed. Since the behaviour of slab track structures are different from conventional ballast railways, new model techniques have been developed, and their behaviour under moving loads has been studied. In this thesis, firstly, 3D finite element model of slab track is created by using ABAQUS software. Further, tools are developed in Excel to investigate the dynamic behaviours under slab track, which is utilized the input of ABAQUS software. Twelve models is developed to examine the effect of material properties used in slab track designs on its behaviour and the responses of all layers under static loading is analyzed. Besides, the effect of train speeds on slab tack behaviour is also evaluated by combining with static analysis data. The results show that the choice of stiff railpad has a significant positive effect on displacement; however, it causes more acceleration of the slab layer. Elastic modulus of soil under the slab layer is a governing factor for vibration frequency, vertical displacement, horizontal stress in the model used concrete sub-slab and vertical stress in the model used asphalt slab. On the other hand, it is generally not crucial for change in the acceleration of layers. Apart from the classical slab track designs, It has been observed that the choice of asphalt material in the sub-slab does not cause any adverse consequence in many parameters examined, which are displacement, acceleration of the layers, stress and vibration. Although the use of asphalt in the lower slab layer causes a limited increase in vertical displacement and vertical stress, there is a moderate decrease in vibration frequency and longitudinal stress values. When regarding the acceleration values, close results are found in the concrete sub-slab.

Statement of Originality

This is to confirm that this is my own work and does not break the University, Department or module conventions on plagiarism as outlined in the current Faculty Academic Misconduct training test.

Mehmethan Oncel

04/09/2020



List of Contents

Abstract	i
Statement of Originality	ii
List of Contents	iii
List of Figures	v
List of Table.....	vii
Abbreviation	viii
Acknowledgements.....	ix
1 Introduction	1
1.1 Research Aims & Objectives	1
1.2 Study Limitations	2
2 Summary of Literature Review	3
2.1 Type of Slab Track	3
2.1.1 Embedded Sleeper.....	3
2.1.2 Non-Embedded Sleeper	3
2.1.3 Monolithic in situ	3
2.1.4 Precast.....	3
2.1.5 Embedded Rail	3
2.1.6 Asphalt Layer	4
2.2 Structural Requirements of Slab Track	5
2.2.1 Subsoil	5
2.2.2 Superstructure	6
2.3 Vibrations and noise	6
2.4 Track deterioration and maintenance	7
2.5 Track modelling	8
3 Methodology	14
3.1 Assumptions.....	14
3.2 Simulation procedure.....	14

3.2.1	Parts and Property	15
3.2.2	Interaction.....	17
3.2.3	Mesh.....	19
3.2.4	Load and Boundary Condition.....	19
3.3	Dynamic analysis calculation method.....	20
4	Models and Numerical Results	22
4.1	Model Development.....	22
4.2	Static Analysis Results	23
4.2.1	Displacement	23
4.2.2	Vertical Stress.....	27
4.2.3	Horizontal Stress	32
4.3	Dynamic Results	34
4.3.1	Acceleration	34
4.3.2	Displacement	39
4.3.3	Vibration properties	42
5	Discussion and Conclusion	46
5.1	Discussion	46
5.2	Conclusion.....	49
5.3	Future Research.....	50
6	References.....	51

List of Figures

Figure 2-1 Type of Slab Track (Freudenstein, 2010).....	4
Figure 2-2 Schematic plan of the requirements for layers (SSF Ingenieure, 2010)	5
Figure 2-3 Comparison of the calculated and experimental velocity at speed of 298 km/h a) at sleepers, at free field at a distance of: b) 3m c)8m d)11 m (Galvín et al., 2010)	9
Figure 2-4 Comparison of the time history of the wheel-rail contact force with the non-linear contact model for different speed a) 350km/h b)300 km/h c)250 km/h d)200 km/h (Lei et al., 2016)	10
Figure 2-5 Simulated finite element model(Nsabimana and Jung, 2015).....	11
Figure 2-6 Vertical displacements along with the model in the subsoil for train speeds between 100 km/h and 300 km/h a) $E_{(subsoil)}=60$ MPa b) 100 MPa (Nsabimana and Jung, 2015)	12
Figure 2-7 Comparison of the displacement under static loading ad dynamic loading for different train speeds a) $E_{(subsoil)}=60$ MPa b) 100 MPa (Nsabimana and Jung, 2015).....	12
Figure 2-8 The 2.5D finite element model of the slab track system (Bian et al., 2011)	13
Figure 2-9 One quarter car model (Bian et al., 2011).....	13
Figure 3-1: Layer dimension of Railway track.....	15
Figure 3-2: Whole Slab track model.....	16
Figure 3-3 Surface to surface discretization (left), node to surface discretization (right) (Connolly, 2013)	18
Figure 4-1 Impact of different stiffness of soil and railpad on vertical displacement a) for models using concrete material in lower slab b) for models using asphalt material in lower slab	25
Figure 4-2 Impact of different materials in the lower slab and different stiffness of soil on vertical displacement a) for railpad stiffness of 80 kN / mm b) for railpad stiffness of 250 kN / mm	25
Figure 4-3 Impact of different stiffness of soil and rail pad on vertical soil stress a) for models using concrete sub-slab b) for models using asphalt sub-slab.....	30
Figure 4-4 Impact of different materials in the lower slab and different stiffness of soil on vertical soil stress a) for railpad stiffness of 80 kN / mm b) for railpad stiffness of 250 kN / mm	30

Figure 4-5 Variation of the vertical stress responses on the bottom of the HBL layer for different models 31

Figure 4-6 Horizontal stress results in the longitudinal direction for models produced using concrete material in the lower slab layer 33

Figure 4-7 Horizontal stress results in the longitudinal direction for models produced using asphalt material in the lower slab layer..... 33

Figure 4-8 Change of acceleration throughout the track for all layers 35

Figure 4-9 Comparison of rail acceleration along the track..... 38

Figure 4-10 Comparison of CBL layer acceleration along the track 38

Figure 4-11 Maximum vertical displacement a)Slab layer for soil stiffness of 120 MPa 41

Figure 4-12 Comparison of the wave velocities plotted against the different train speed a)for slab layer b) for top of the soil 44

List of Table

Table 2-1 The maximum wheel-to-rail contact forces (Lei et al., 2016)	10
Table 2-2 Displacement and acceleration values of layers for different velocities for linear contact mode	10
Table 2-3 Material properties (Nsabimana and Jung, 2015)	11
Table 3-1: Material Properties of Railway Track	16
Table 3-2 Master and Slave Surfaces for interaction.....	18
Table 3-3 Mesh size of each layer.....	19
Table 4-1 Description of developed model properties	23
Table 4-2 Maximum vertical displacement (unit is mm) in the rail for all models	24
Table 4-3 Maximum vertical displacement (unit is mm) in the CBL for all models	27
Table 4-4 Maximum vertical stress (S22) in the top of the soil layer for all models	28
Table 4-5 Horizontal Stress for both direction for all models	33
Table 4-6 Calculated maximum acceleration (m/s^2) in all layers at train speed of 250 km/h for a different model	35
Table 4-7 Calculated maximum acceleration (m/s^2) in all layers for different train speed (Model 1)	35
Table 4-8 Calculated maximum acceleration (m/s^2) in all layers for different train speed (Model 7)	35
Table 4-9 Maximum vertical displacement result for all model a)Slab layer b)Soil	42
Table 4-10 Calculated wave frequencies in examined models for different train speed a) for slab layer b) for a top of the soil.....	45
Table 4-11 Calculated wave velocities in examined models for different train speed a) for slab layer b) for a top of the soil.....	45

Abbreviation

Acc	Acceleration
ATD	AsphaltTragschicht mit Direktauf Lagerung - Asphalt rail span with direct support
BEM	Boundary Element Method
BL	Bound Layer
CAM	Cement Asphalt Mortar
CBL	Concrete Base Layer
Disp.	Displacement
FE	Finite Element
FEM	Finite Element Model
FEM	Finiti Element Method
FPL	Frost Protection Layer
HBL	Hydraulically Bound Layer
LVT	Low Vibration Track
MBS	Multibody System

Acknowledgements

I would like to express sincere gratitude to my supervisor, Dr Nick Thom, for his advices and guidance regarding the thesis and the railway industry, which was very valuable for me, his patience, support, and immense knowledge. I would like also to thank to Mucahit Atalan for helping me on almost every subject and his time spent for me during my studies.

I would like to represent my appreciation to all my friends in Turkey, especially Batuhan Çınar, Esin Damar, Göktañ Aydınçđ, Mustafa Tekinli and Semih Yılmaz who are always in there whenever I need them even if they're thousands of miles away. Without their support this experience would have been very difficult. I cannot thank all of them enough.

Further thanks go to my colleagues with whom I studied together all term and my flatmates with whom I have had great experiences and friendship.

I would like to thank the Republic of Turkey, the Ministry of National Education for providing me scholarship and supporting my studies during my entire education in UK.

Finally, first and foremost, my most special thanks are due to my lovely family. I would like to express my endless gratitude to my mother, Halime Öncel, who has always believed in me and is my safest shelter in my life. I would like to thank my father Osman Öncel, my sisters Derya Özgür and Cennet Öncel Sipahi for their support during this journey. I would also like to thank Salim Özgür and Sefer Sipahi for all their help.

1 Introduction

With the development of the railway sector, train speeds started to increase, and high-speed train lines started to be built. The reduce in the travel time between the cities, more comfortable and punctual journeys allow the demand for the high-speed train to increase. However, dynamic forces and vibration induced by the increase in speed may cause the track structure to deteriorate. This deterioration may lead to derailment or other unfavourable consequences. It requires improvement and frequent maintenance of the railway embankment to keep the track uniform at high speeds.

One way to improve track performance is to increase granular layer thicknesses, but this is not an effective way. Moreover, it also needs frequent maintenance. The other alternative solutions, known as slab track was developed. In this method, it is used to prefabricate or in-situ slab instead of the ballast layer.

The use of slab track in high-speed trains is becoming widespread throughout the world. Although this design has disadvantages such as initial cost, adjustment of the slab, it has many benefits that cannot be overlooked for track stability. Using slab track enable the more stiffness layer and prevent fouling caused by the ballast layer. As a result, rising strength of track-bed, lower maintenance cost and long service life may provide the performance of track-bed to increase.

1.1 Research Aims & Objectives

In this thesis, the aim is to analysis the slab track behaviour under static and dynamic loading as well as investigating the effect of material properties on the response of slab track. The results obtained may help to provide preliminary information about the materials considered to be used in slab design. To achieve this, the following objectives need to be fulfilled.

- Developing tools that simulate the dynamic behaviour of slab track realistically by using static analysis results.
- Evaluation of the displacement and stress results at the top of the ground level, under the rail and slab layer.
- Assess the effect of different train speeds on acceleration and vibration by considering various material properties.

In this direction, this project consists of five main chapters. In the first part, the background and research aims & objectives are introduced, the literature research is summarized in the second part, the method followed by the modelling and tools developed in Excel are explained in the third part, the models and their results are presented in the fourth part, and the last part contains discussion and conclusion sections.

1.2 Study Limitations

The main limitation in this thesis is that the university computer with the full version of the ABAQUS software on which the model will be done could not be delivered due to COVID-19, so this study was carried out with a limited number of nodes in the student version of ABAQUS. For this reason, the model had to be downsized considerably. While considering the 16-meter-long track model (the whole track in the transverse direction), half of the model was made for eight meters by using the symmetry feature of the slab tracks. Additionally, sleepers that were thought to be used as embedded in the CBL layer were removed since they increased the number of mesh considerably and the rail was directly tied to the CBL layer with the railpads. Even the model was made as small and simple as possible due to limited number of nodes, the number of mesh used in the model were a lot less than it should be. Thus, the layers could not be meshed perfectly, which is crucial in models calculated using the finite element method.

The dynamic analysis method was not preferred in this study as the time given for the completion of the project was limited. In almost all subjects studied on the slab track, it is tried to reflect the rail-wheel interaction in the best way to obtain more realistic results. However, this causes the calculation time to increase considerably, which this study did not have enough time to do this. For this reason, a dynamic interpretation has been attempted by using static analysis data, which led to results that are incompatible or unexpected with the literature in some sections.

2 Summary of Literature Review

2.1 Type of Slab Track

2.1.1 Embedded Sleeper

A concrete layer is used instead of the ballast layer, and the sleepers are embedded in the concrete layer. The casting of the concrete layer and sleepers used for adjustment of track geometry is done simultaneously. If the track geometry needs to be re-adjusted, this results in a lot of labour and cost. Rheda 2000 and Züblin are examples of this system (Matias and Ferreira, 2020).

2.1.2 Non-Embedded Sleeper

In this system, sleepers are covered with the elastomeric hull, which provides high flexibility and noise protection, and resilience pad is used under the sleepers. While sleepers and other supporting elements are easy to exchange, there is a possibility of water seeping into the elastomeric hull. LVT used in Switzerland is a successful example of this system (Michas, 2012).

2.1.3 Monolithic in situ

This method is applied by using a continuous monolithic concrete layer. This system enables a rigid and stiff slab design and acts as an elastic beam of the slab under traffic loading. This system, which allows the load to spread over a wider area, makes it suitable for use in poor foundations (Esveld, 2001).

2.1.4 Precast

In this category, in which direct fixing systems are preferred, slabs are produced as reinforced or pre-stressed concrete and assembled on concrete or asphalt roadbed. Using precast method provide high construction efficiency due to labour-saving and quick renovation and maintenance. However, construction far from the manufacturing area is costly due to logistics expenses. This method is applied in Shinkansen and Bögl systems (Matias and Ferreira, 2020).

2.1.5 Embedded Rail

Rail fixing is done by enclosing all rail elements except railhead with the elastic compound. This system provides excellent rail support and reduces noise productions (Esveld, 2001).

2.1.6 Asphalt Layer

In this method, sleepers are placed on the asphalt layer instead of a concrete slab. The system called ATD in Germany consists of an asphalt layer on the concrete roadbed. It allows higher track elasticity regardless of foundation stiffness. This system not only facilitates the adjustment of the track geometry but also increases the track elasticity. However, it is not appropriate to use it in places with extreme weather conditions (Michas, 2012).

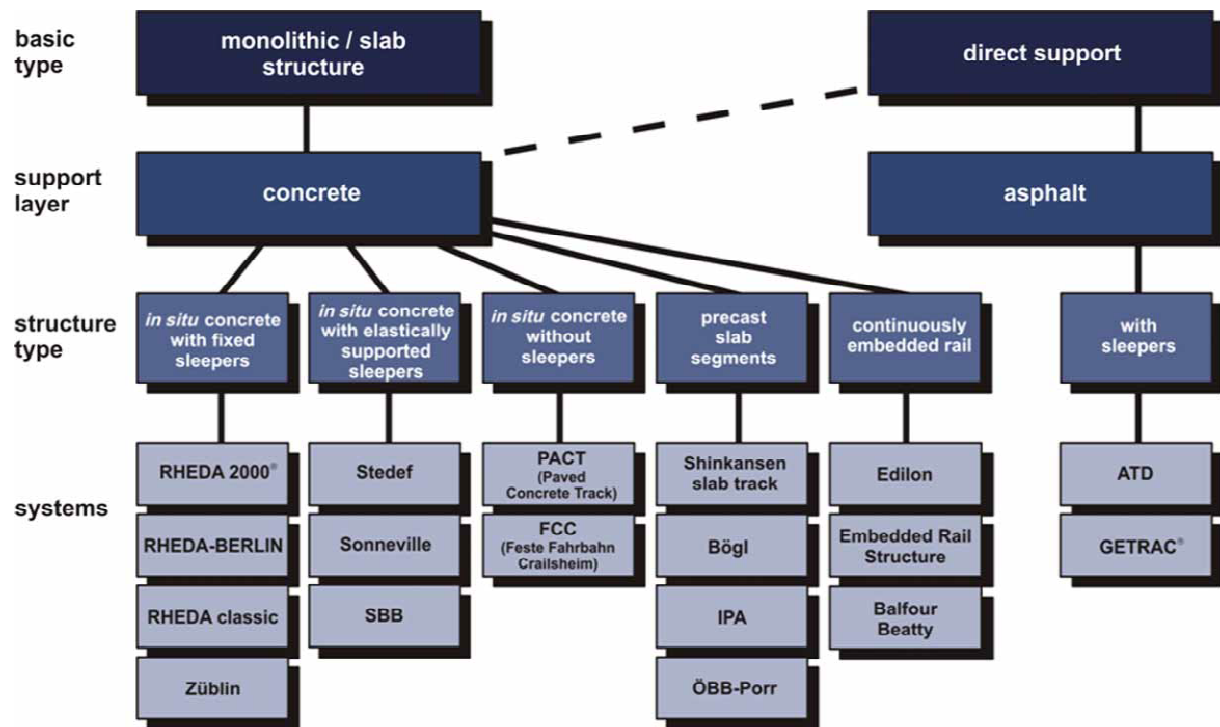


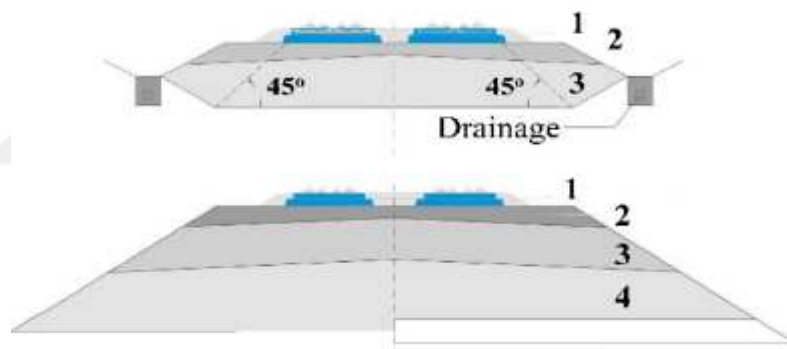
Figure 2-1 Type of Slab Track (Freudenstein, 2010)

2.2 Structural Requirements of Slab Track

2.2.1 Subsoil

One of the critical factors affecting the slab design is the foundation soils. The occurrence of different settlements on the grounds affects the project life of the slab. Therefore, these settlements must remain within certain limits. Acceptable limit, according to Japanese standards, is 12.5 mm for a 20-meter chord (Zhu and Cai, 2011). Several studies have been done to determine the reasonable settlement limitation (Duan et al., 2016). Zhang et al. (2016) developed a vehicle- track dynamic model considering the weight of track structure to examine the subgrade differential settlement.

In the slab design, it is required to fulfil some requirements on the soil. German standard is generally applied (Matias and Ferreira, 2020). The minimum values for the layers are shown in Figure 2-2.



1 Hydraulic bonded layer 2 Frost protection layer ($E_{v2} \geq 120$ MPa)

3 Subgrade material ($E_{v2} \geq 60$ MPa & $h > 3$ m) 4 Subgrade material ($E_{v2} \geq 45$ MPa)

Figure 2-2 Schematic plan of the requirements for layers (SSF Ingenieure, 2010)

2.2.2 Superstructure

Structural designs of slab track systems are made by considering temperature or load distribution, which are two primary concern. Since modular slab is used in Japanese designs, there is no load distribution between them. For all reasons, the most critical issue in Japanese's system is the trainload that the track will be exposed to rather than the temperature. On the other hand, Continuous slab track is preferred in German's design. The major concern in these kinds of tracks is imposed deformation caused by temperature changing (Liu et al., 2011). In order to limit the crack widths that may occur in slabs, reinforcements are generally used on the neutral axis. Whereas the bending stiffness is thought to be higher, they can be placed eccentrically (Steenbergen et al., 2007). Cho et al. (2014) investigated the effect of the quantify of steel bars and the location on the crack widths and tensile stress under environmental influences. As a result, the increase in the steel bar ratio decreases the width of the cracking. It contributes significantly to the stress distribution, which extends the performance life of the track.

2.3 Vibrations and noise

The damping and elasticity properties of the structure are the components used to characterize the natural frequencies and vibration modes of ballastless systems (Matias and Ferreira, 2020). Some studies have been conducted to examine the effects of vibration behaviour on the entire track. Lei (2017) developed the finite element model representing the dynamic behaviour of the ballastless system and investigated the impact of different track elements on the track. At the end of the study, it was found that the rail pads have little effect on track displacement. However, the vibration on the overall track structure is immensely influenced by the change of the subgrade stiffness. The dynamic index of track components decreases in subgrade layers with higher stiffness.

It is also studied to reduce ground-borne vibration in ballastless systems. Floating slab track designs would be efficient for loads above 10Hz frequency. Kuo et al. (2008) found that the use of stiffer rail clips would be subject to higher wheel-rail contact force. Using soft stiffness designs decrease the outgoing vibration, but it causes more vibration and deflection in slabs and rail components.

Another disadvantage of slab tracks is that they are 2-4dB noisier than ballasted tracks (Thompson and Gautier, 2006). Noise problems are more important in viaducts than open plain tracks. To solve this problem, Cooper and Harrison (2002) designed an alternative viaduct design using a floating rail slab track with soft rail fasteners.

2.4 Track deterioration and maintenance

The increasing physical deficiencies of the track cause fatigue and structural deterioration. The sources of these problems are various; concrete slab damages, soil settlements, fastening problems and rail wear are the main reasons.

CAM is used in slab tracks to provide roughness between concrete base and slab. Moreover, it absorbs a significant amount of vibration and provides comfort for fast-speed vehicles (Zhu et al., 2014). Degradation of this layer under high traffic load causes some problems. Damage of this layer due to high traffic load tends to create voids under the slab. Ren et al. (2016) discovered that the deterioration of the CAM layer adversely affects the carrying capacity on the bearing capacity.

Moreover, Zhu and Cai (2014) studied the damage that occurred in the interface between the slab and CAM layers due to changing of temperature and investigated their effect on the slab track dynamic behaviour. As a result, this situation causes cracking and delamination. A similar investigation was also done by Song et al. (2014). They found that if the slab is exposed to high temperatures and the mortar layer is damaged, its effect on track dynamic properties is negligible. This indicates that the track can remain in the appropriate geometric shape.

2.5 Track modelling

Experimental and numerical researches have been conducted to analyze the dynamic behaviour of slab track. The development in the modelling process has become increasingly complex and models have begun to be designed with more different methods. First, dynamic loads were solved by means of differential equations, and analytical methods were developed for this (Warburton, 1976). They were replaced by finite element method, as they were insufficient especially in areas especially where track - vehicle interaction was examined (Lei, 2016). FEM, which was first used in elastic foundation beams (Frýba et al., 1993), was later used in 2D and 3D models (Auersch, 2006). One of the drawbacks of FEM is that it is not suitable for modelling the soil. For this reason, it is aimed to obtain more realistic results by combining different methods such as Galvín et al. (2010)'s study (eg BEM and MBS). In the following section, different modelling methods and research findings conducted previously are summarized.

Bian et al. (2014) and Wang et al. (2017) performed full-scale testing in the laboratory. While Bian et al. (2014) obtained the results of the dynamic soil-structure interaction and the effect of the train speed on the line structure, Wang et al. (2017) found dynamic stiffness and dumping coefficient for the four different slabs designed using a mathematical model.

Although models for ballast railways are very advanced, these models are not suitable for slab tracks. Since the vibration and mechanical behaviours of the two models are completely different, new models have been developed (Matias and Ferreira, 2020). Galvín et al. (2010) studied on a three-dimensional model using boundary element method (BEM), the multibody system (MBS), and finite element method (FEM). The vehicle is modelled as MBS. While the FEM method was used for track structure, the BEM method was used for soil modelling. As a load, only the trainload was taken into consideration. The numeric model made was verified comparatively with the experimental data on the existing Cordoba-Malaga high-speed line. Computed results and experimental results were found to be quite similar and are shown in Figure 2-3.

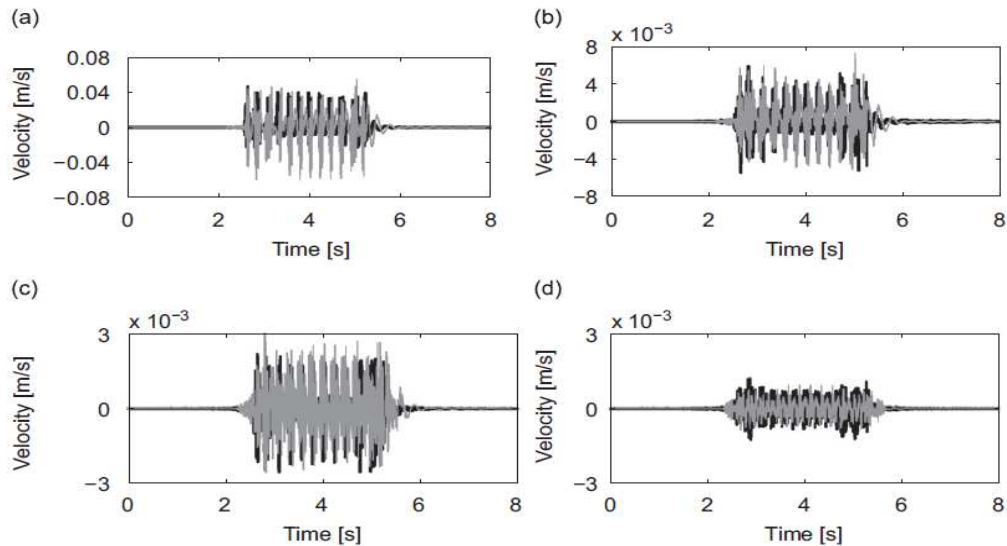


Figure 2-3 Comparison of the calculated and experimental velocity at speed of 298 km/h a) at sleepers, at free field at a distance of: b) 3m c)8m d)11 m (Galvín et al., 2010)

On the other hand, Lei et al. (2016) solved the modelling with a different approach and achieved his results in a shorter time. They developed a model for the dynamic analysis of the vehicle-track non-linear coupling system by using the FEM. The dynamics equations of the vehicle-track non-linear coupling system were solved using the cross iteration algorithm and relaxation technique. Thus, so the calculation time was greatly reduced. At the end of the study, it was found that as the train speed increased, wheel-rail contact forces, acceleration and vertical displacement of the layer (rail, CBL and HBL) also increase. Moreover, linear and non-linear models have been developed to investigate the effects on rail wheel contact force. Maximum wheel-rail contact force with a linear model is higher than the non-linear approach. Results are given in Figure 2-4, Table 2-1, Table 2-2.

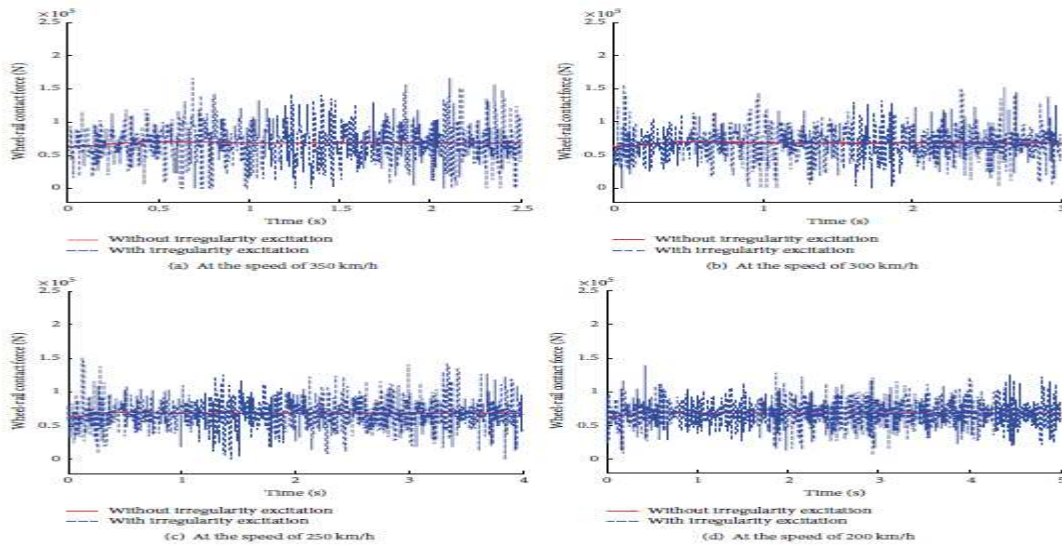


Figure 2-4 Comparison of the time history of the wheel-rail contact force with the non-linear contact model for different speed a) 350km/h b)300 km/h c)250 km/h d)200 km/h (Lei et al., 2016)

Speed (km/h)	Wheel-to-rail linear contact (kN)	Wheel-to-rail nonlinear contact (kN)
350	172.38	166.31
300	160.05	152.16
250	142.41	141.95
200	122.53	125.80

Table 2-1 The maximum wheel-to-rail contact forces (Lei et al., 2016)

Train Speed/ Layer	Rail		CBL		HBL	
	Acc. (m/s ²)	Disp. (mm)	Acc. (m/s ²)	Disp. (mm)	Acc. (m/s ²)	Disp. (mm)
350	1216	-1,9	40,83	-1	37,07	-1
300	897	-1,7	29,89	-0,95	29,17	-0,89
250	337	-1,6	26,21	-0,77	28,56	-0,74
200	240	-1,4	21,98	-0,7	21,92	-0,67

Table 2-2 Displacement and acceleration values of layers for different velocities for linear contact mode

On the other hand, Nsabimana and Jung (2015) modelled it as a simplified method. The 2D finite element method was advanced to investigate the dynamic response of the reinforced concrete slab line to different ground stiffness and various train speeds. All components used in the model were considered to be linear elastic. The track structure and properties of each material are shown in Figure 2-5 and Table 2-3 respectively.

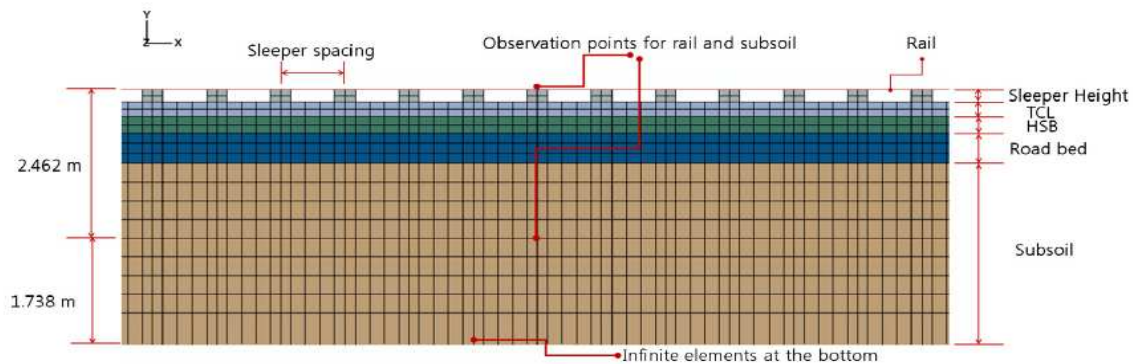


Figure 2-5 Simulated finite element model(Nsabimana and Jung, 2015)

Component	Mass density, ρ (ton/m ³)	Stiffness ^a	Poisson's ratio, ν	Thickness	Coefficients of the Rayleigh damping model
Rail	7.8	$E = 210$ GPa $I = 3055$ cm ⁴	0.3	-	-
Sleeper	2.3	$E = 29.1$ GPa	0.2	20 cm	$\alpha = 3.6779$ sec ⁻¹ $\beta = 2.33 \times 10^{-5}$ sec
TCL	2.3	$E = 34.0$ GPa	0.2	24 cm	
HSB	2.3	$E = 12.9$ GPa	0.2	28.4 cm	
RB	2.0	$E = 180$ MPa	0.2	50 cm	
Subsoil	2.0	$E = 60$ MPa	0.3	2.976 m	

^a E = Young's modulus, I = Moment of Inertia.

Table 2-3 Material properties (Nsabimana and Jung, 2015)

Rayleigh damping was defined to the finite element model for the dynamic simulation of the running train. The two parameters of Rayleigh damping are determined by the formula below.

$$\alpha = \frac{2\xi\omega_1\omega_2}{\omega_1 + \omega_2} \quad \text{and} \quad \beta = \frac{2\xi}{\omega_1 + \omega_2}$$

Where ζ is damping ratio, ω_1 and ω_2 are angular frequencies.

The vertical displacements obtained for the different train speeds in the subsoil layers with 60 MPa and 100 MPa stiffness are shown in Figure 2-6.

Figure 2-7 illustrates the maximum vertical displacements resulting from dynamic and static loading at different speeds for the two different ground stiffness.

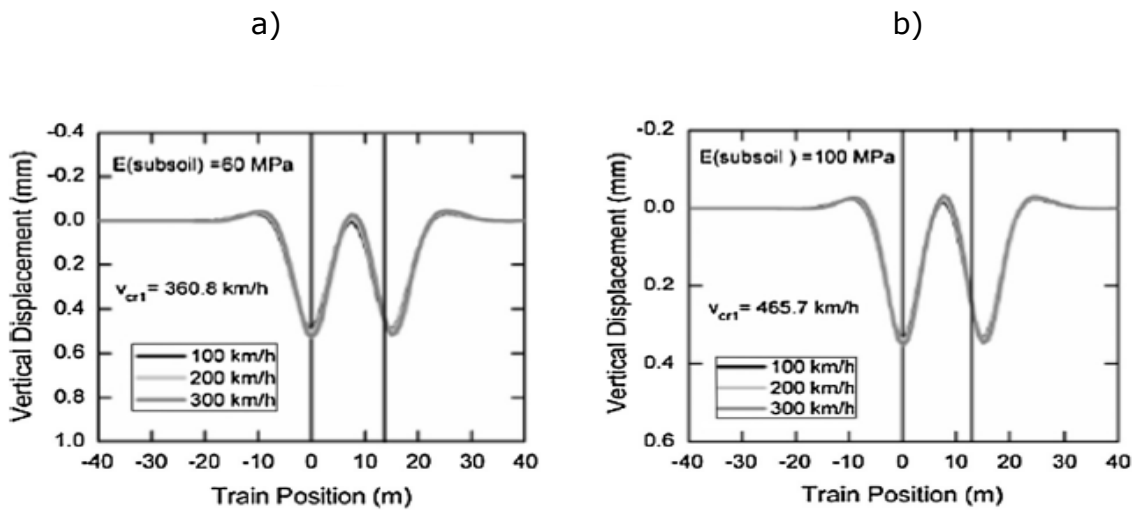


Figure 2-6 Vertical displacements along with the model in the subsoil for train speeds between 100 km/h and 300 km/h a) $E(\text{subsoil}) = 60 \text{ MPa}$ b) 100 MPa (Nsabimana and Jung, 2015)

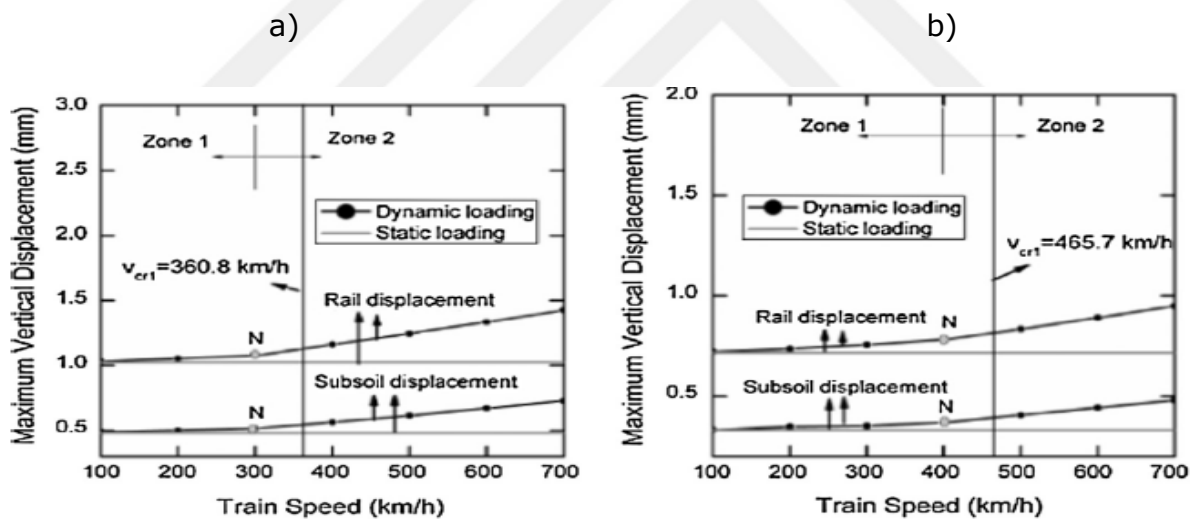


Figure 2-7 Comparison of the displacement under static loading and dynamic loading for different train speeds a) $E(\text{subsoil}) = 60 \text{ MPa}$ b) 100 MPa (Nsabimana and Jung, 2015)

Bian et al. (2011) developed modelling based on the 2,5D finite element method, which analyzes the dynamic interaction between the train-track-ground to predict ground vibrations caused by vertical track irregularities.

The dynamic response of the track caused by the movement of the train was obtained by resolving the governing equations in the wave-number domain. The cosine distribution with amplitude and wavelength was used to represent irregularities at the rail surface. The values of u_c , u_b , u_w are used to represent the vertical movement of the vehicle's body, bogie and wheels. The interaction forces of the train while travelling at c speed is described by the formula below.

$$\begin{aligned} \bar{q}(\omega - \zeta_x c) &= W_1 \delta(\omega - \zeta_x c) + W_2 \delta(\omega - \omega_1 - \zeta_x c) \\ &\quad + W_3 \delta(\omega + \omega_1 - \zeta_x c) \\ &= \frac{1}{c} \sum_{i=1}^3 W_i \delta\left(\zeta_x + \frac{\omega - \omega_i}{c}\right) \end{aligned}$$

Equation 2-1

Dynamic loading resulting from irregular movement of the train is provided with Equation 2.1.

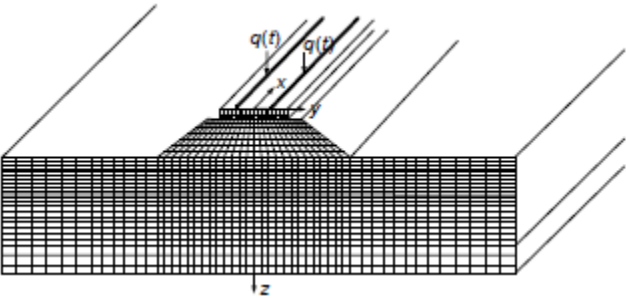


Figure 2-8 The 2.5D finite element model of the slab track system (Bian et al., 2011)

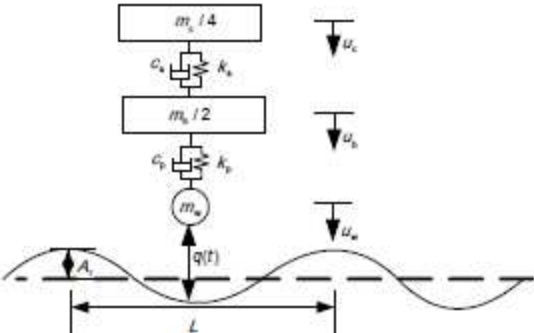


Figure 2-9 One quarter car model (Bian et al., 2011)

Lei and Zhang (2011) presented the model to obtain the dynamic analysis of the vehicle-track-ground coupling system by deducing the relevant mass matrix, stiffness matrix and damping matrix. The mathematical method was developed using the Lagrange equation, and the related finite element matrix was formulated to combine the moving wheel and rail with the formula.

3 Methodology

In order to examine the displacements, vertical and horizontal stresses occurring under static loads, and to calculate the acceleration, amplitude and wavelengths of vibration induced from high-speed trains utilizing static analysis results, a 3D railway track model was developed using the commercial program ABAQUS which is the FE (Finite Element) Software.

3.1 Assumptions

While developing the model, the following assumptions are made;

- The linear elastic assumption was used in the analysis of the structure. It means, when the load has disappeared, the structure retakes its initial form.
- Another assumption is isotropicity. Material properties for each component were precisely the same in every single direction.
- Settlements that may occur in the soil were not considered. This approach is highly acceptable in soils with high bearing capacity. This assumption is one drawback of the finite element method and static analysis (Prakoso, 2017).
- Viscous behaviour was not taken into account in models using asphalt under the concrete layer.

3.2 Simulation procedure

Although the 3D model dimensions designed are based on Rheda 2000, which is the most preferred slab track system in Germany (Michas, 2012), there are some differences. Since the slab track systems are symmetrical, half of the track is modelled. Thus, computation time can be decreased. The frost protection layer (FPL) was not used as the bearing capacity of the examined soil is high (Young's modulus for a different structure is 120, 90 and 60 MPa respectively). Lastly, the rail is tied directly to the upper concrete base layer (CBL) with the railpad without using a sleeper.

In this project, twelve different models have been developed by using soil with different modulus, railpad with different stiffness and two kinds of materials under the concrete layer to examine the effect of material properties on the structure.

3.2.1 Parts and Property

Parts modulus is used to generate the component of railway track. Each layer was created separately, which are rail, railpad, concrete base layer (CBL), hydraulically bound layer (HBL) (bound layer was used in some structures) and soil. In this thesis, all components were created as a deformable solid element. The rail has been designed as a rectangular section with 150 mm wide and 135 mm high, which is the same second-moment inertia as the UIC60 rail profile. Figure 3-1 shows the dimensions of each layer of the model. The entire 3D model, designed for 8.1 m in length, is shown in Figure 3-2.

The material properties were determined by compiling from similar studies conducted earlier. Slab track component parameters for the finite element model are summarized in Table 3-1.

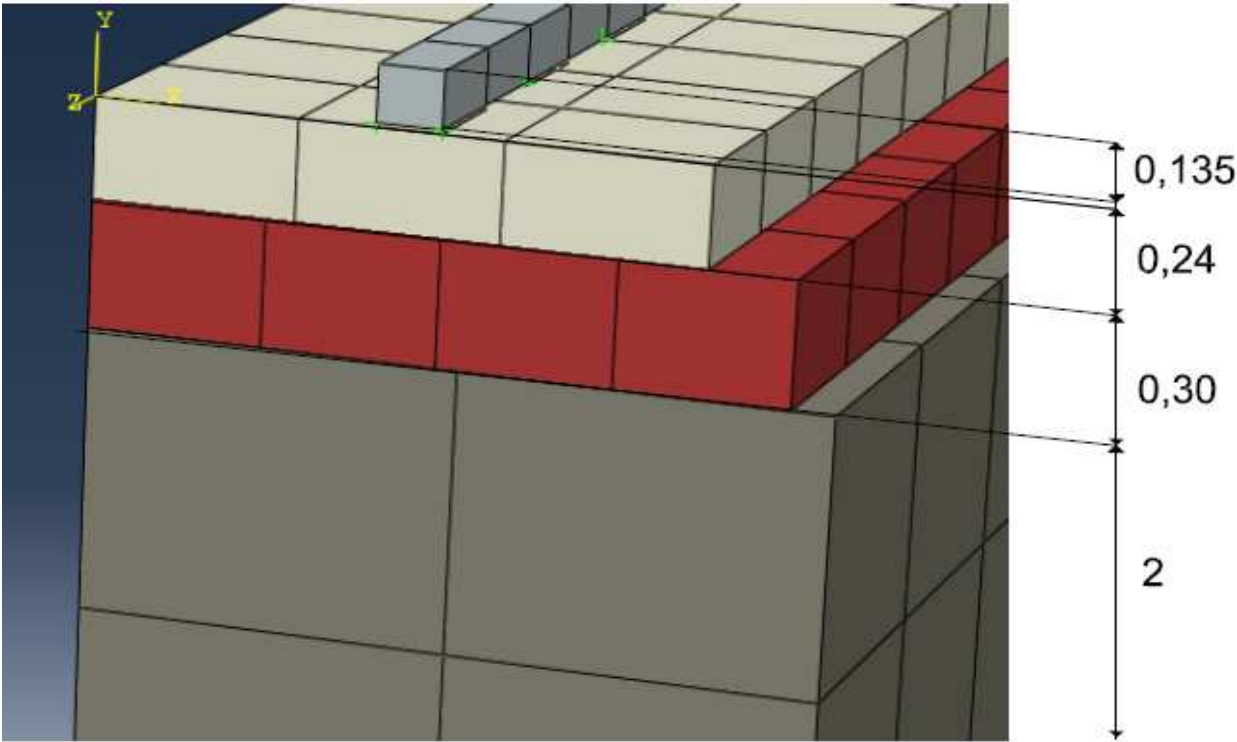


Figure 3-1: Layer dimension of Railway track

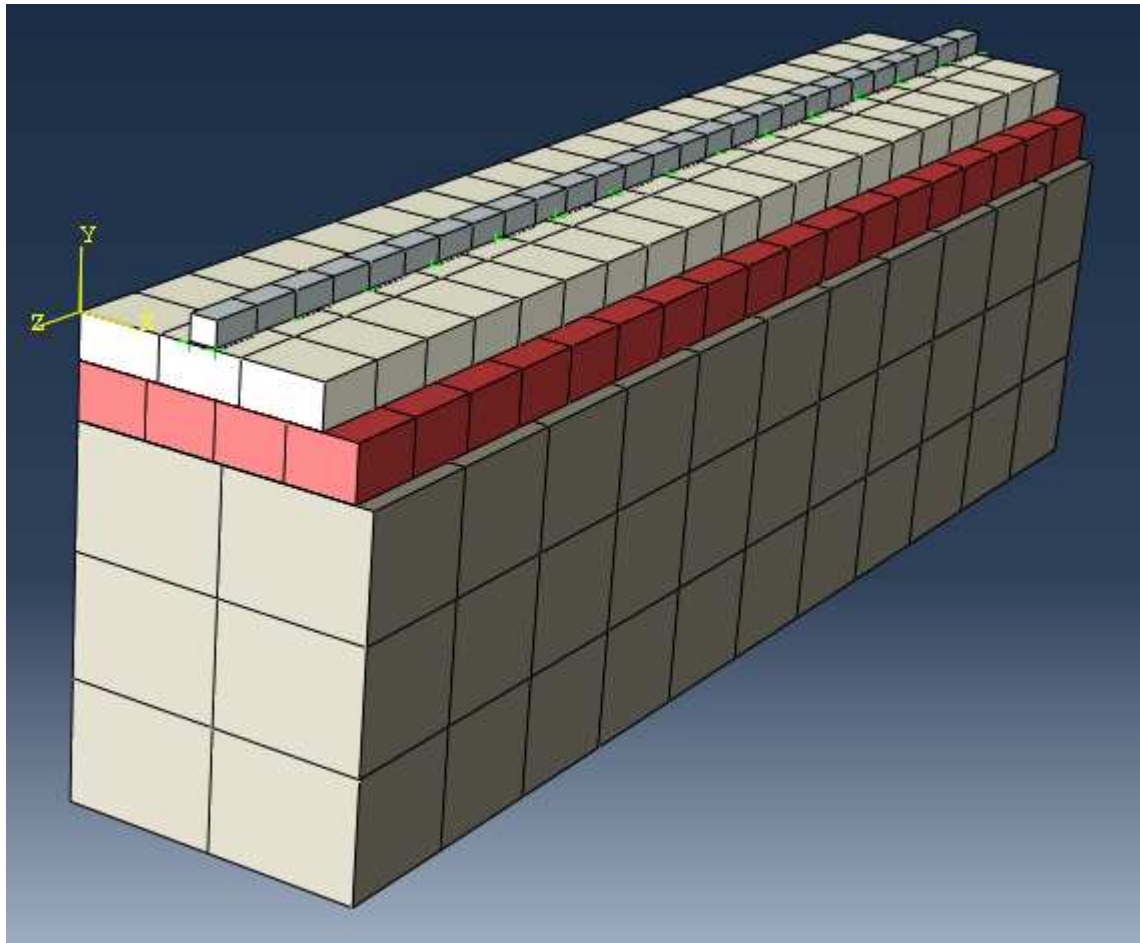


Figure 3-2: Whole Slab track model

Material	Unit Weight (kg/m ³)	Dimension(m)		Young's modulus (E)	Poisson's ratio, ν
		Width	Height		
rail	7850	0,15	0,135	210 GPa	0,3
concrete layer	2400	1,4	0,24	34 GPa	0,2
hbl(concrete)	2400	1,6	0,3	12,9 GPa	0,2
bl(asphalt)	2350	1,6	0,3	5 GPa	0,35
soil (1)	2000	1,7	0,666	120 MPa	0,3
soil (2)	1950	1,7	0,667	90 MPa	0,35
soil (3)	1950	1,7	0,667	60 MPa	0,35
railpad (1)	1950	0,15	0,01	17,78 MPa	0,01
railpad (2)	1950	0,15	0,01	55,56 MPa	0,01

Table 3-1: Material Properties of Railway Track

In this study, railpads with 80 kN /mm and 250 kN /mm stiffness values were used. Since the material property should be defined as Young's Modulus in ABAQUS, these stiffness values were converted to Young's Modulus with the formula below;

Railpad dimensions; 150 mm × 10 mm × 300 mm (width, thickness, length)

$$\text{For } 80 \text{ kN/mm} \rightarrow \frac{80 \times 10^3 \text{ N}}{150 \text{ mm} \times 300 \text{ mm}} = 1,778 \text{ MPa per } 1 \text{ mm deflection}$$

$$\text{For } 10 \text{ mm deflection for } 10 \text{ mm thickness railpad; } \frac{1,778}{0,1} = 17,78 \text{ MPa}$$

If we assume that 10 mm represent a strain of 1; 17,78 MPa equal the modulus of railpad with 80 kN/mm.

$$\text{For } 2500 \text{ kN/mm} \rightarrow \frac{250 \times 10^3 \text{ N}}{150 \text{ mm} \times 300 \text{ mm}} = 5,556 \text{ MPa per } 1 \text{ mm deflection}$$

$$\text{For } 10 \text{ mm deflection for } 10 \text{ mm thickness railpad; } \frac{5,556}{0,1} = 55,56 \text{ MPa}$$

Since the railpad is a kind of texture, the Poisson's ratio is zero. Therefore, Poisson's ratio is defined as 0.01 to the software.

3.2.2 Interaction

Identifying the interaction of each layer in a realistic way is an essential factor in ensuring the validity of the model.

In this model, the interaction between the layers is defined by the type of 'tie constraints' contract used by Connolly (2013) and Shih et al. (2017) in their work.

The surfaces that are connected to each other are defined in two different ways as slave surface and master surface in Tie constraint. In this thesis, master surface was selected according to the following priorities;

- The surface having larger mesh has been chosen as master surface,
- If the mesh size of surfaces is identical, the surface of the bottom layer was selected as a master surface.

Considering the above criteria, master surfaces for the contact between layers are listed in Table 3-2.

	Master Surface	Slave Surface
Between Soil and HBL	Soil	HBL
Between HBL and CBL	HBL	CBL
Between CBL and Railpad	CBL	Railpad
Between Railpad and Rail	Railpad	Rail

Table 3-2 Master and Slave Surfaces for interaction

In Tie Constraint, there are two discretization methods which are called surface to surface and node to surface. Surface to surface discretization method, which gives better convergence and contact stress results, was used in all contacts except between railpad and rail (Shih et al., 2017). Node to surface was used between railpad and rail. This method is preferred since railpads are not continuous like other components. Surface to surface and node to surface constraints methods are shown in Figure 3-3.

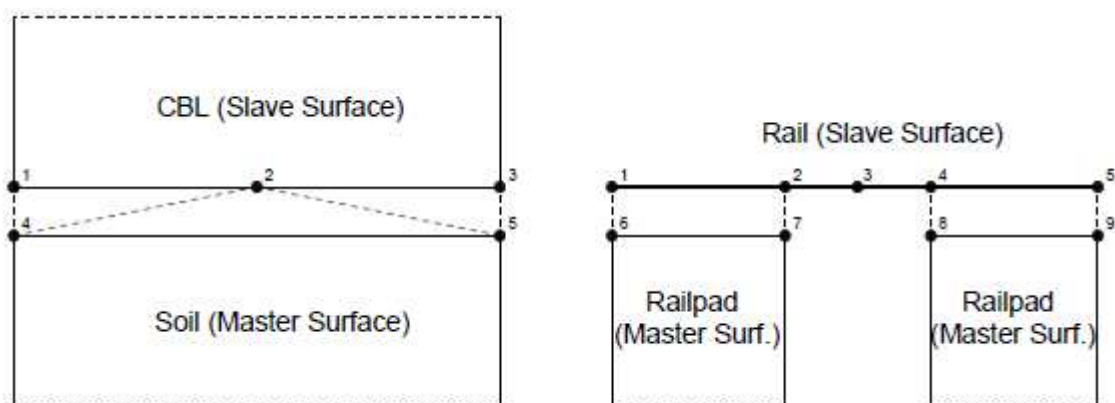


Figure 3-3 Surface to surface discretization (left), node to surface discretization (right) (Connolly, 2013)

In addition, although it can be considered in properties such as contact damping, thermal conductivity, only normal and tangential behaviour is taken into consideration in this study.

3.2.3 Mesh

In the analyzes made using the finite element method, element sizes are vital for obtaining more realistic convergence. Although fine mesh gives you more accurate results, it increases the calculation time considerably. That is why it is crucial to find the optimum mesh size. The best way to keep the relationship between precision and computation time at the optimum level is to use different mesh sizes taking into account the position of the structure (Arañó Barenys, 2016). While fine mesh was preferred in places where the geometry is complex such as the interaction of the rail and the railpad, the load is applied, the coarse mesh was used in simpler structures and large parts such as soil.

The element sizes used are summarized in Table 3-3 for each layer.

Layer	Mesh Size		
	Horizontal (m)	Longitudinal (m)	Vertical (m)
Rail	0,15	0,3	0,135
Railpad	0,15	0,3	0,01
CBL	0,467	0,405	0,24
HBL	0,4	0,45	0,30
Soil	0,85	0,736	0,667

Table 3-3 Mesh size of each layer

3.2.4 Load and Boundary Condition

In this study, since the static analysis is carried out, it was defined as a single load of 55 kN at the beginning of the model. According to the UIC code, 22.5 t axle load is allowed on D type lines, which equates to 220 kN. In this study, since 1/4 of the rail track was modelled, the load applied to the model is 55 kN. Thus, it remained on the safer side by analyzing the track with maximum force.

Loads can be applied to nodes and surfaces in two different ways. In order to represent the interaction between the load and the structure more accurately and to obtain more precise results, the load was applied to the surface defined on the rail, similar to the Arañó Barenys (2016) study.

For symmetry properties to be accurately represented in the model, boundary conditions should be appropriately defined. In this study, boundary conditions were used in four regions. These are the beginning section of the structure where the load is applied, left side of the model, below the soil layer and each railpads.

All layers on the side where the load is applied are restricted in the longitudinal direction (z direction), while the rotation in all directions is released. At the same time, no restrictions were used at the end of the model. Since half of the railway track is modelled, the left side of the CBL, HBL and soil layers is fixed in the transverse direction, which is a boundary condition in the x-direction. Moreover, each railpad is limited in the longitudinal direction. As the soil is buried in reality, it was represented by restricting the freedom in all direction including rotation.

3.3 Dynamic analysis calculation method

When the static analysis is performed, the acceleration of the object is ignored, which is the main point that distinguishes dynamic analysis from static analysis. Slab's up and down movement causes resistance force. This is what is taken into account in dynamic analysis every time. This extra stress causes the deflection value to change. In this section, how dynamic behaviour results are calculated in Excel using static analysis results are explained.

Vertical stress value, width and mass values of the layer examined on the prepared spreadsheet were taken from the results of Static analysis as input. Since stress results in ABAQUS can be obtained according to mesh nodes, this value varies between 0.3 and 0.75m, which means a huge time interval, input stress values were interpreted to correspond every 10 cm. Force/m was obtained by multiplying the corrected stress value by width. With Equation 3-1 and Equation 3-2, acceleration value was calculated for each x distance.

$$a = \frac{F}{m} \text{ and}$$

Equation 3-1

$$F = F/m - k \times y + \zeta \times v$$

k: spring stiffness

y: maximum displacement from ABAQUS

ζ : damping ratio

v: velocity

Equation 3-2

When force is calculated, spring force and damping were simply taken into account. Spring stiffness was chosen based on the static analysis results; while the damping ratio was accepted as 0.4 (0.4 was accepted as an example without any evidence).

The velocity value was calculated by integrating the acceleration value, and the displacement value under dynamic effect was calculated by integrating the velocity. Thus, the behaviour of the track under dynamic conditions was calculated approximately.

After the displacement under dynamic effects was calculated, the frequency and speed of the wave produced by the train were calculated with the deflection value under dynamic analysis. For this, the following assumptions were made.

- It is assumed that the shape of the wave resembles that of the stress applied against x . Thus, the wavelength of the wave could be estimated.
- The point where ' $\lambda \cdot x$ ' = $\pi/4$ was calculated by using the beam on elastic foundation equation.

The period of the wave was found by determining the time difference between where the each deflection peaked and the frequency of the wave was calculated by the Equation 3-3. Then, after calculating the wavelength of the wave with the second assumption, the speed of the wave produced by train was calculated with the formula in Equation 3-4.

$$f = \frac{1}{T}$$

Equation 3-3

$$V = \lambda \times f$$

v = speed of the wave; λ = wavelength of wave; f = frequency (Hz)

Equation 3-4

With the methods and assumptions described in this section, the vibration characteristics produced by the train could be estimated for slab and ground. Since the time interval in the spreadsheet is quite large for the vibration frequency occurring on the rail, the dynamic effects on the rail could not be examined. Since the upper and lower slab will move together, the properties of the two layers have been combined to determine the vibration characteristics.

4 Models and Numerical Results

This part presents the development of different models and analysis of layers displacement, vertical and horizontal stress result obtained by using static analysis in ABAQUS as well as the dynamic effect under the track which is simulated utilizing the static analysis results in Excel.

In the first part, the differences between the developed models are explained. In the second section, the data obtained as a result of static analysis were examined, and the effect of the changed material properties on the structure was discussed. In the third section, dynamic results produced by using the existing data are presented and compared for different models.

4.1 Model Development

Recently, different slab track designs have been developed using various component properties and different type of material to get excellent ride quality, reduce the effect of vibration induced high-speed train on the soil and prevent possible lower base cracking. Generally, a concrete layer is used in the upper and lower layers. In some case, the asphalt base layer is preferred instead of concrete in both layers. In this study, four basic designs were developed, and each design was examined with three different soil stiffness. In whole models, rail designed as a rectangular shape which is the same second-moment inertia with UIC60 rail profile with 210GPa Young's modulus was used and top slab base were designed as concrete with 34 GPa Young's Modulus. In the main model which is called model no 1, a concrete with 12,9 MPa modulus were preferred in the lower slab layer, while 80 kN /mm soft railpad stiffness were used under the rail. The behaviour of this model on stiff soil (120 MPa) was investigated. Model 2 and 3, which have the same features as Design 1, were examined for 90 MPa and 60MPa modules soils, respectively. In the second basic design, in order to analyze the results of using concrete and asphalt together in slab tracks, the concrete layer in the lower slab was replaced with asphalt. At the same time, the other features were preserved, and the design was analyzed for three different soil classes (Model No 3,4 and 5). The difference between the other two basic designs is the use of a stiffer rail pad. Basic design three was obtained by replacing the 80 kN/mm softer railpad used in basic design one with 250 kN/mm. Basic design four is similarly produced from basic design two by changing railpad stiffness. The models and material properties are summarized in Table 4-1.

Design No	1			2			3			4		
Layer/ Model No	1	2	3	4	5	6	7	8	9	10	11	12
Pad Stiffness	80 kN/mm						250 kN/mm					
Concrete Base Modulus	34 GPa											
HBL/BL Material and Modulus	concrete base (12,9 GPa)			asphalt base (5 GPa)			concrete base (12,9 GPa)			asphalt base (5 GPa)		
Soil Modulus	120 MPa	90 MPa	60 MPa	120 MPa	90 MPa	60 MPa	120 MPa	90 MPa	60 MPa	120 MPa	90 MPa	60 MPa

Table 4-1 Description of developed model properties

4.2 Static Analysis Results

In this section, the displacement and stress graphs obtained as a result of static loading of twelve slab track models designed by changing the material properties are illustrated.

4.2.1 Displacement

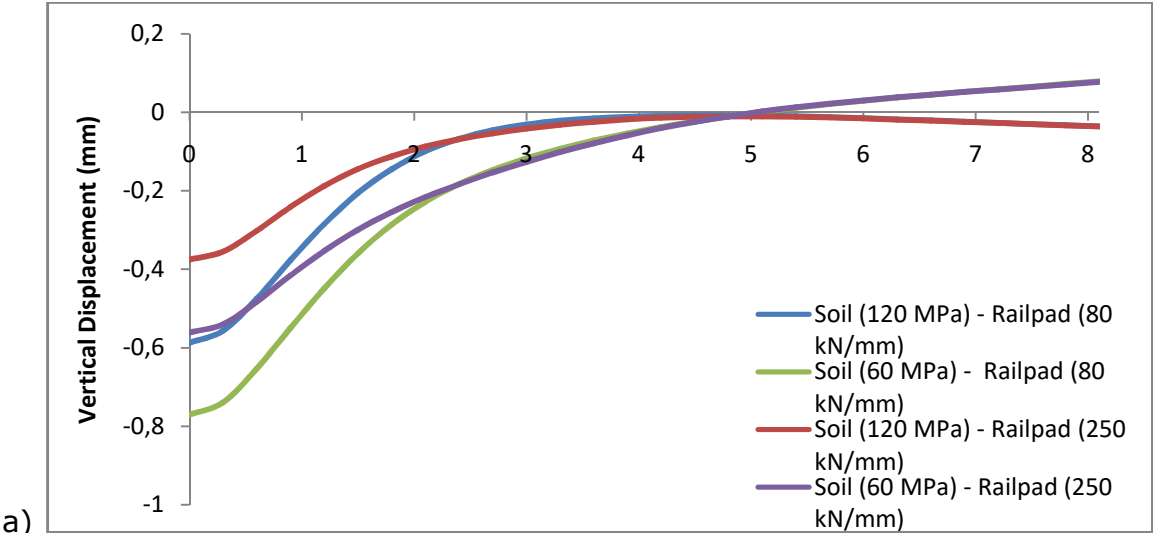
Due to the reasons explained in Section 3.3, the dynamic behaviours occurring in the rail could not be examined. Therefore, the outputs calculated by the FEM as a result of the static loading of the models developed in the ABAQUS software are presented. The dynamic responses of the slab track obtained with the tools developed in Excel are shown in the dynamic analysis chapter 4.3 for the slab layer and the soil, as well as the comparison of their dynamic behaviour with different models.

The displacement results is taken from the nodes on the railpad, under the rail layer. Since the mesh dimensions are 30 cm, the displacement graphs for the rail are drawn using the outputs of every 30 cm distance from the point where the load is applied to the end of the model. Figure 4-1 shows how the eight designed models behave differently under static load. Since the models using soils with 90MPa Young's modulus behave similarly to soils with 120 MPa stiffness, their displacement results are not compared on the graph. Their maximum displacement results are presented in Table 4-2 together with the other models. Figure 4-2, the same models in Figure 4-1 are presented to show the effect of the material used in the slab layer on the behaviour of the track.

As can be seen from Figure 4-1, Figure 4-2 and Table 4-2, railpad stiffness and soil stiffness are the main factors affecting the displacement at rail, while the use of concrete or asphalt in the lower slab appears to be relatively less effective, which asphalt and concrete give almost the same results on softer soil. This because the asphalt and concrete are both very stiff material and spread the load properly. As the concrete spreads the load partially better, a limited decrease is observed in the displacement values in basic designs 1 and 3 using concrete compared to models using asphalt with similar properties. Another reason can be that there is no change in the stiffness of the upper slab layer, which is the main layer that is exposed to more loads and reduces deformation by distributing the load. If asphalt were used in the upper and lower pavement layers, the displacement values would probably be higher than the slab track models where concrete and asphalt is used together.

Design/ Soil Stiffness	120 MPa	90 MPa	60 MPa
Design 1	0,587048	0,622202	0,770401
Design 2	0,658974	0,729154	0,767956
Design 3	0,374821	0,409819	0,561167
Design 4	0,454274	0,521947	0,563467

Table 4-2 Maximum vertical displacement (unit is mm) in the rail for all models



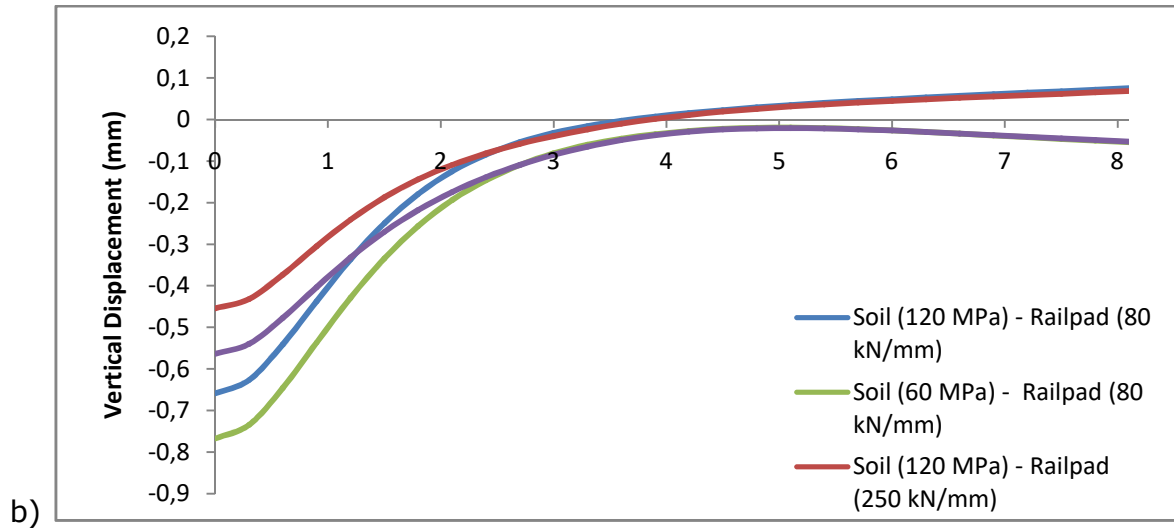


Figure 4-1 Impact of different stiffness of soil and railpad on vertical displacement a) for models using concrete material in lower slab b) for models using asphalt material in lower slab

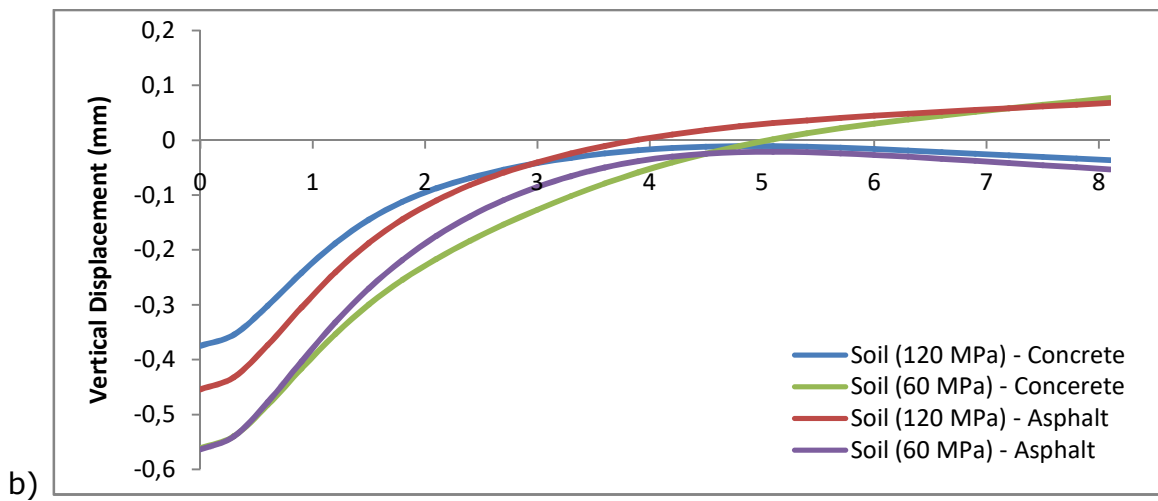
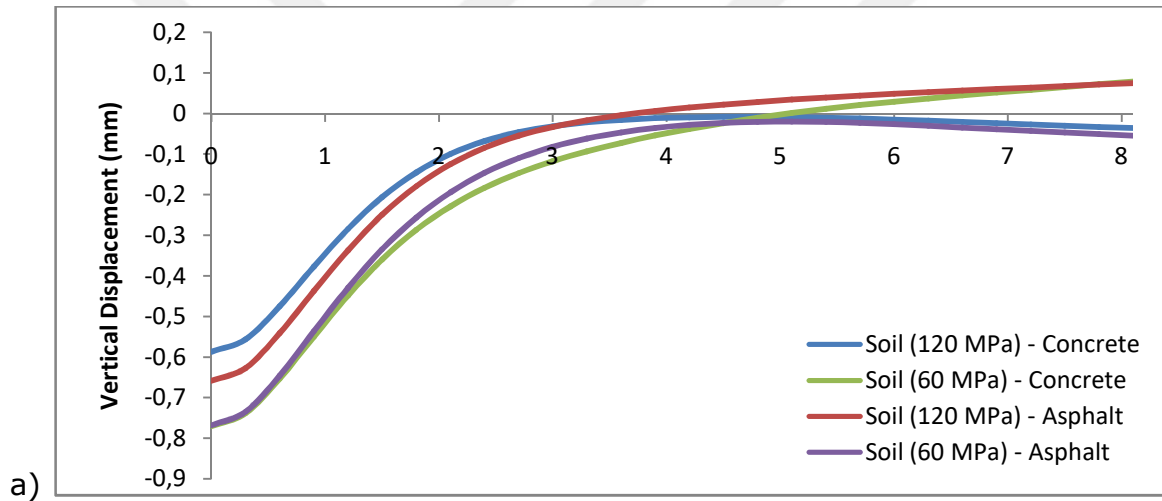


Figure 4-2 Impact of different materials in the lower slab and different stiffness of soil on vertical displacement a) for railpad stiffness of 80 kN / mm b) for railpad stiffness of 250 kN / mm

In railway track design, it is aimed to prevent excessive displacement that may occur in places where the stiffness of soil is low by preferring harder railpad. In this study, the vertical displacement in rail decreases significantly in the models where harder railpads are used together with the soil having low Young's modulus. The vertical displacement value of 0.77 mm in Model 3 and 6 (lower soil stiffness and softer railpad) decreases by about 27% to 0.56 mm for Model 9 and Model 12, which is very close to model 1 and model 4 designed by using softer railpad and stiff soil. In addition, quite reasonable results have been obtained in terms of displacement in models with harder rail pads and soil having high Young's modulus. Vertical displacement value of 0.59 mm and 0.66 mm in Model 1 and Model 4 decrease to 0.37 and 0.45 mm, respectively, by replacing the 80 kN / mm railpad used in these models with 250 kN / mm. However, there is some trouble caused by the use of harder railpads at the track. Railpads are used to reduce displacement as well as to reduce the level of track vibration. However, this low vibration situation may result in resonance with structures near the railway, is not the desired situation (Connolly et al., 2015). The effect of harder railpad usage on track vibration frequency and vibration speed will be analyzed in section 4.3.3 vibration results. In addition, when the impact of the railpad on the displacement of the CBL layer is examined, the opposite of the effect seen on the rail is seen in the CBL layer. While increasing railpad stiffness decreases the displacement in the rail, it increases the displacement in the CBL layer in a limited way. This may be caused by the larger central force acting on the CBL layer. It is seen that the maximum vertical displacement value in all models in designs 3 and design 4, where 250 kN /mm railpads are used, is around 3% - 4% higher when compared to models with the same features except the railpad stiffness in designs 1 and design 2. The displacement values in the CBL layer for all models are shown in Table 4-3.

It is observed that the use of soil with Young's modulus of 60 MPa in the basic design 1 and 3, where concrete sub-slab is used, significantly increases the displacement. The displacement value of 0.37mm in Model 7 reached 0.56 mm with a significant increase of 50% in Model 9. On the other hand, this ratio varies between 17 percent and 24 percent in models using asphalt sub-slab. The displacement of 0.66 mm in Model 4 increases to 0.76 mm with only 17 percent increase. The reason for the significant increases observed in designs using

concrete sub-slab may be due to sudden changes in the soil stiffness. While the concrete stiffness used in the models is 12.9 GPa, this value is only 60 MPa in softer soil, which indicates a serious difference between the two layers. In areas where slab track application will be made, if the soil is soft, FPL (Frost Protection Layer), which is an intermediate layer, can be made in these sections to reduce the load on the soil and reduce the displacement under the rail. In addition to this, since the use of asphalt material instead of concrete in the lower slab give similar result in terms of vertical displacement and stress (will be explained next section), as well as when considering the ease of construction and cost-benefit of asphalt, concrete - asphalt slab track designs can also give very efficient results without using an intermediate layer in places with lower stiffness soil.

Design/ Soil Stiffness	120 MPa	90 MPa	60 MPa
Design 1	0,207296	0,243043	0,394018
Design 2	0,283784	0,353332	0,3952
Design 3	0,214582	0,250207	0,401181
Design 4	0,294816	0,363233	0,406913

Table 4-3 Maximum vertical displacement (unit is mm) in the CBL for all models

4.2.2 Vertical Stress

Soil stresses in railway infrastructure are one of the essential signs taken into consideration in railway track design. Excessive stresses occurring in this layer may cause extra deformation. Thus, in addition to the decrease in the ride quality of the line, frequent maintenance may be required. For this reason, determining the stress on the ground surface is very crucial for proper railway design. (Bian, Jiang et al.2014). Soil stresses occurring as a result of static loading on the central axis along the ground surface with the finite FEM have been performed for different models. Maximum stress values obtained from the ABAQUS software are summarized in Table 4-4.

The static stress on the ground surface varies between 13-20 kPa for different models, and these results are very close to the dynamic analysis results obtained in both field tests and different software (Chen, Zhao et al.2013, Lamas-Lopez, Cui et al.2017). Considering this situation, it can be said that the static analysis results can give similar results to the models that simulate the real situation better as going down the slab surface.

Design/ Soil Stiffness	120 MPa	90 MPa	60 MPa
Design 1	14,87 kPa	13,97 kPa	14,24 kPa
Design 2	18,57 kPa	18,52 kPa	14,69 kPa
Design 3	15,34 kPa	14,32 kPa	14,48 kPa
Design 4	19,21 kPa	18,96 kPa	15,08 kPa

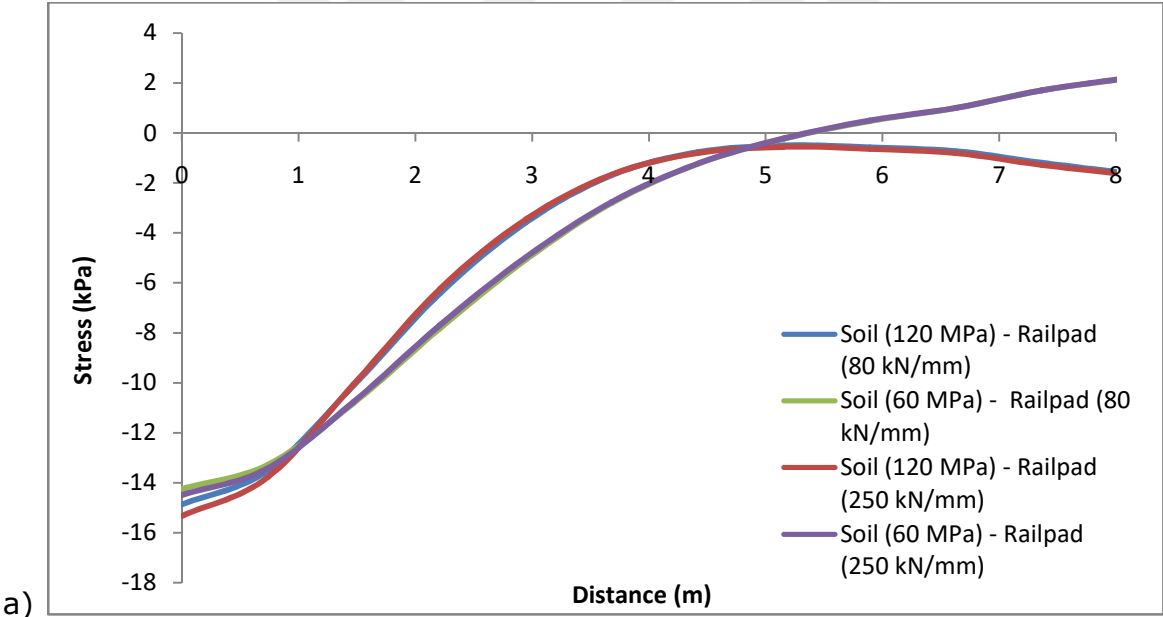
Table 4-4 Maximum vertical stress (S22) in the top of the soil layer for all models

Although the stress differences are not much for different soil classes in the basic design 1 and 3 mentioned in Chapter 4.1, 22% less stress was observed in the models having low soil stiffness in the basic design 2 and 4 where asphalt is used at the lower slab layer. While the tensile stress value is 19.21 kPa in model 10 where asphalt sub-slab is used with 120 MPa soil stiffness and 250 kN / mm railpad, it is seen that the vertical soil stress is slightly over 15 kPa in model 12, which has the same properties with Model 10 except soil stiffness ($E = 60$ MPa), the change is only around 5 percent in model generated using concrete sub-slab. The stress values calculated in Model 7 and Model 9 are 15.34 and 14.48 kPa, respectively. The high stresses on stiff soil may be due to their excessive resistance force, which also allows the load to spread over a wider area and reduce the displacement.

It is seen that the stress graph takes a horizontal shape in many models from the fourth meter and the effect of the static load approximately disappears towards the end of the model. On the other hand, in models where concrete is used with softer soil (model 3 and model 9) and models where asphalt is used with harder soil (model 4 and model 10), the stress graph switches to the positive side after approximately fourth meters. The behaviour of these four models mentioned above differently than expected may be due to boundary conditions. The end of the model is freed to see how many meters the load affects the length from the static loading point. Otherwise, the displacement graph at the end of all models would be zero, causing less approximation. This situation may have caused an approximate error in the stress graph results where the effect of the load decreased, and these sections are the parts where the model is less important. Since the designed model represents $\frac{1}{4}$ of the real track, the middle point where the load is applied is essential, and the results obtained at this point give more accurate results.

When the effects of the materials used on the stress distribution is examined, the impact of the difference stiffness of the railpad on the stress distribution is quite limited, whereas the type of material used in the lower slab significantly affect the stress graph. When comparing model 1 and model 7 where only the railpad stiffness is different, the stress value is 14.8 kPa in model 1 with 80 kN/mm railpad stiffness, while this value in model 7 with 250 kN/mm railpad stiffness is only 3.4 percent higher than model 1, which is 15.3 kPa. On the other hand, model 4, in which asphalt sub-slab is used, is approximately 25% more than model 1 using concrete on the lower slab with the same features as model 4. Vertical soil stress in model 4 climbs to 19 kPa.

Figure 4-3 shows the comparison of how the change in soil modulus and railpad stiffness affects stress in models using asphalt sub-slab and concrete sub-slab. The effect of asphalt and concrete behaviour on stress distribution with different soil stiffness is shown in Figure 4-4.



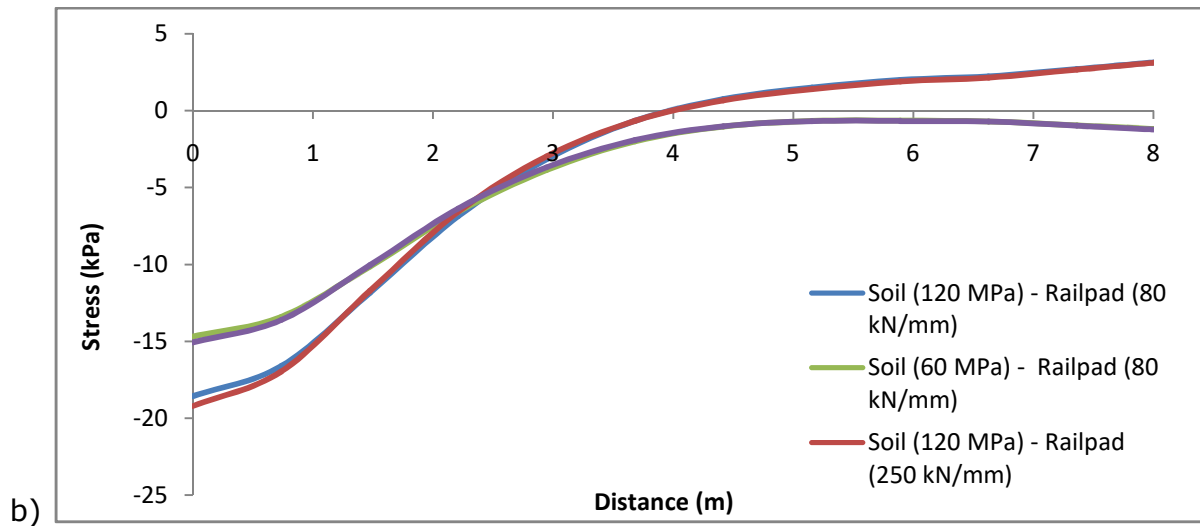


Figure 4-3 Impact of different stiffness of soil and rail pad on vertical soil stress a) for models using concrete sub-slab b) for models using asphalt sub-slab

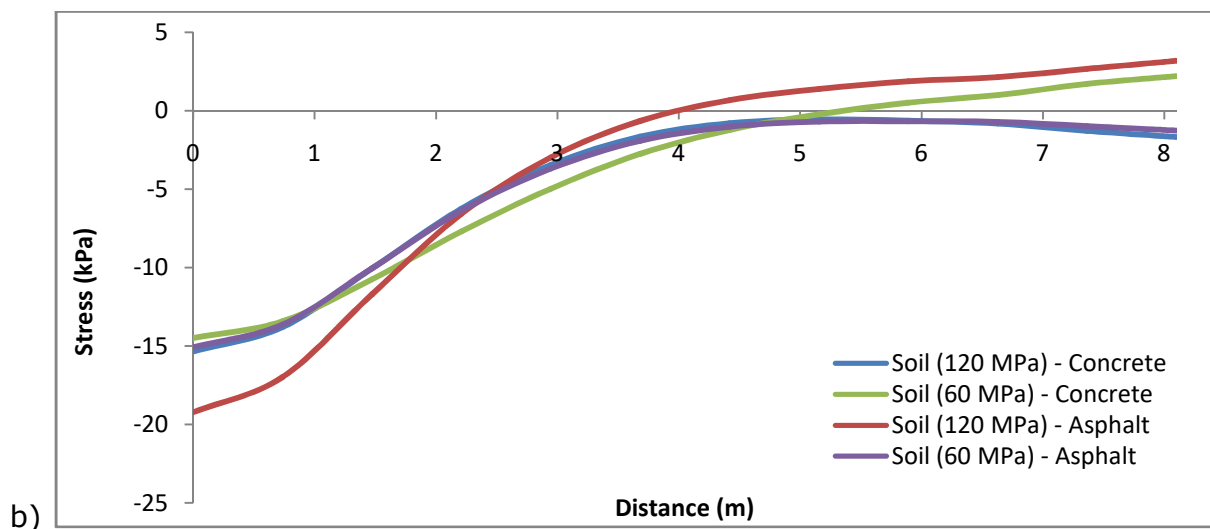
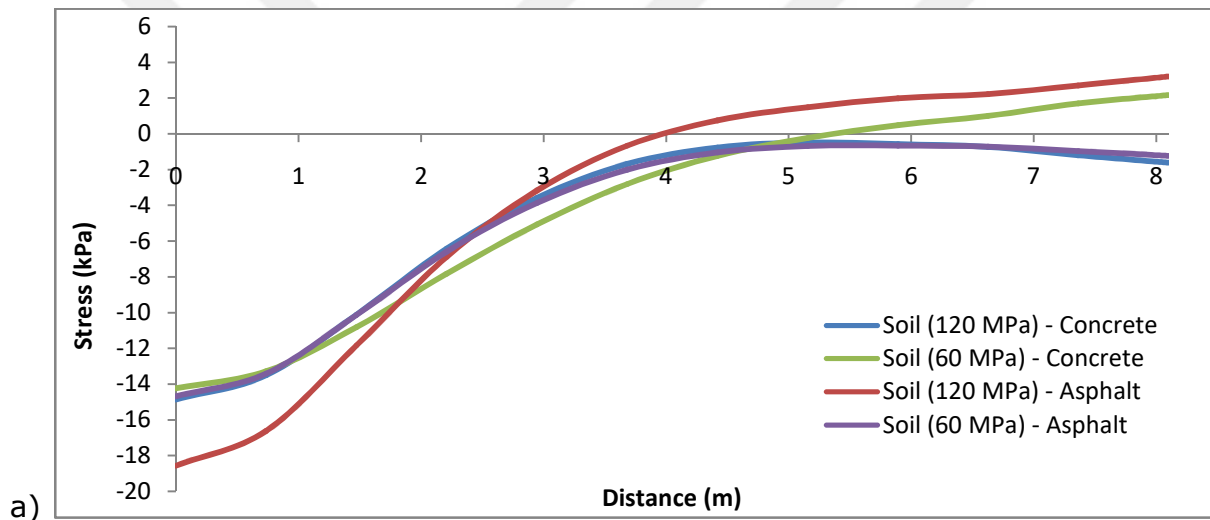


Figure 4-4 Impact of different materials in the lower slab and different stiffness of soil on vertical soil stress a) for railpad stiffness of 80 kN / mm b) for railpad stiffness of 250 kN / mm

When the effect of different materials on the vertical stress in the HBL layer is examined, it is quite similar to the variation in the soil layer. The impact of using a more stiff rail pad on stress, lower stress in models with a lower soil module, and the changes in stress due to the use of concrete or asphalt material in the lower slab is quite similar for the HBL and Soil layer. However, the behaviour of vertical stress across the track is quite different compared to the soil. As seen in Figure 4-5, the stress in the HBL layer demonstrates a very fluctuating motion, which is unexpected for the stress generated as a result of static loading. It is quite possible that this is due to mesh sizes that are not properly adjusted. Due to the student version of the program used in this study, very limited (1000 nodes) nodes could be used, which caused the model to be small and the mesh sizes to be large. The mesh size mismatch between layers may have caused incorrect calculations in the FEM, which is already an approximate method.

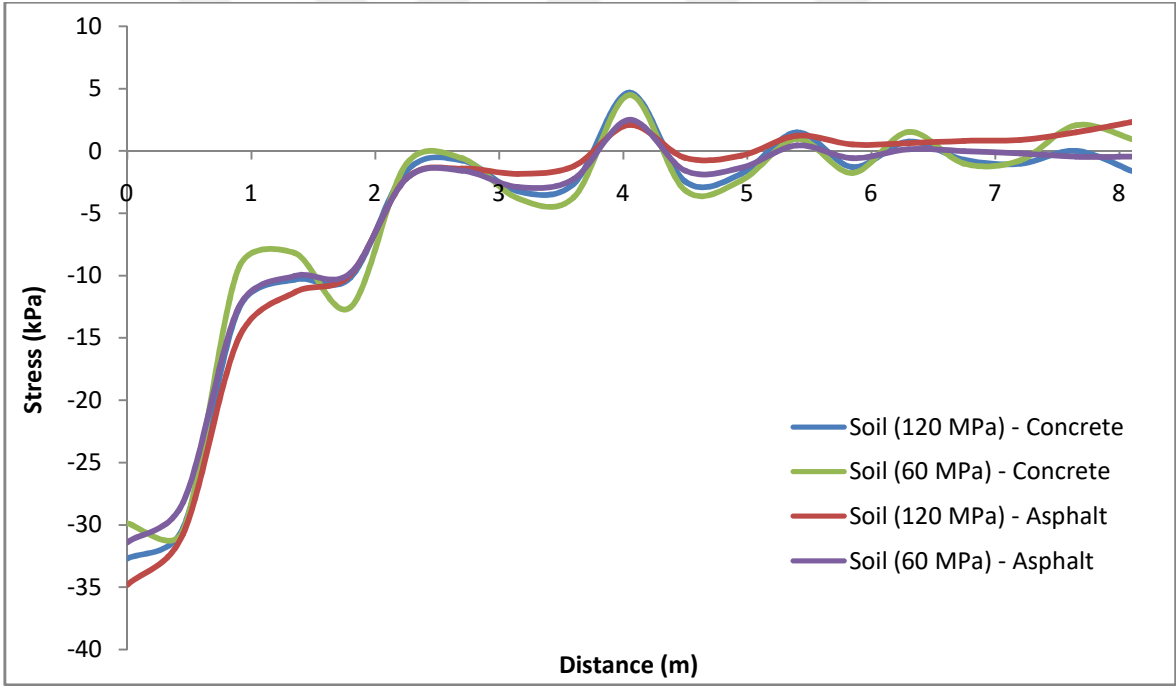


Figure 4-5 Variation of the vertical stress responses on the bottom of the HBL layer for different models

4.2.3 Horizontal Stress

One of the problems that can be encountered in slab track designs is cracks that may occur in the concrete layer. Excessive tensile stresses in the lower concrete layer can cause the concrete to crack and deteriorate the ride quality of the line. In this section, the behaviour of HBL (BL) layer under 55kN static loading was examined. Figure 4-6 and Figure 4-7 show the stress distribution for HBL (BL) in the longitudinal direction of different models designed. Figure 4-6 shows the stress diagram of the models designed using concrete in the lower slab layer, while Figure 4-7 shows the graph of the models using asphalt in the lower slab layer.

It has been observed that the use of concrete slab in soil classes with less stiffness significantly increases the longitudinal stress value. This may be due to the sudden transition from a very stiff layer to a relatively low modulus layer. While the maximum stress value occurring at the point where the load is applied is 177 kPa in model 1 (120MPa soil and 80kN / mm Railpad), it goes up to 300 kPa in model 9 where a stiff railpad (250 kN / mm) and soft soil (60 MPa) is used. However, in the case of using asphalt slab, no serious stress increase was observed with the change of soil stiffness. Longitudinal stress value, which is about 150 kPa in model 4, increases to 200 kPa in model 12. The use of stiffer rail pads do not have much effect on the stress value in both designs (asphalt base and concrete base). There is only a 12% increase in the Model 7 and Model 10 with stiffer rail pad compared to Model 1 and Model 4. The use of asphalt in the lower slab layer offers considerably less stress value compared to models where concrete sub-slabs are used, especially with a soil with low modulus. Considering that asphalt has better strength than concrete against tensile stresses, using asphalt instead of making an FPL layer in areas where the railway line passes through regions with lower ground modulus can give more practical and economic results. In addition, the use of a stiffer railpad can significantly reduce the displacements, and it does not cause a significant increase in the stress value to which the HBL (BL) layer is exposed so that it can be used in places with low modulus soil.

Table 4-5 shows the maximum longitudinal and transverse stress values calculated in all models in the HBL (BL) layer.

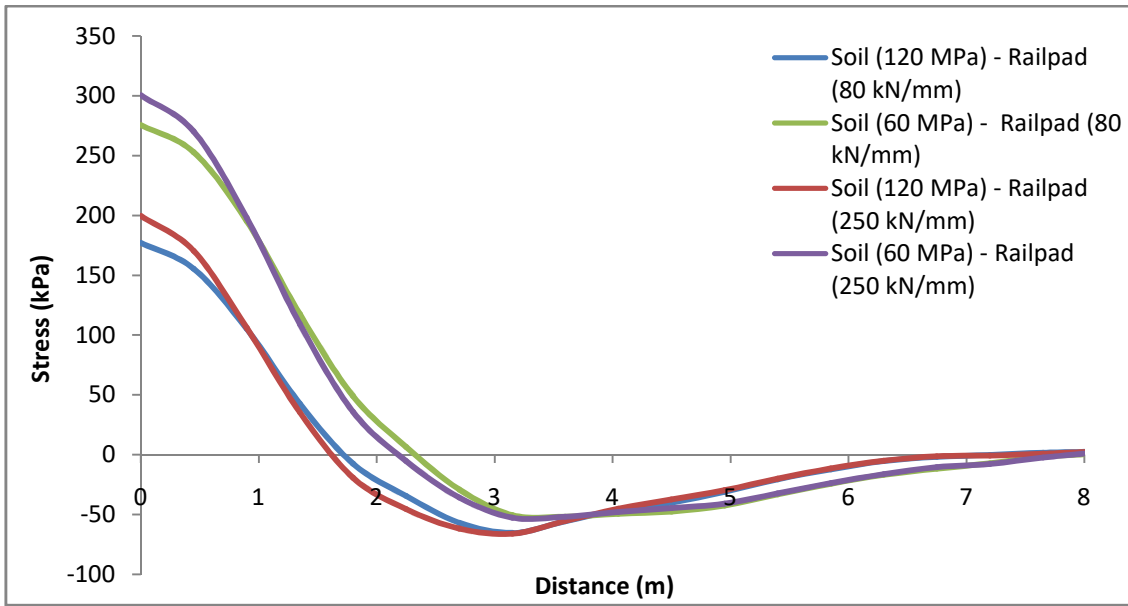


Figure 4-6 Horizontal stress results in the longitudinal direction for models produced using concrete material in the lower slab layer

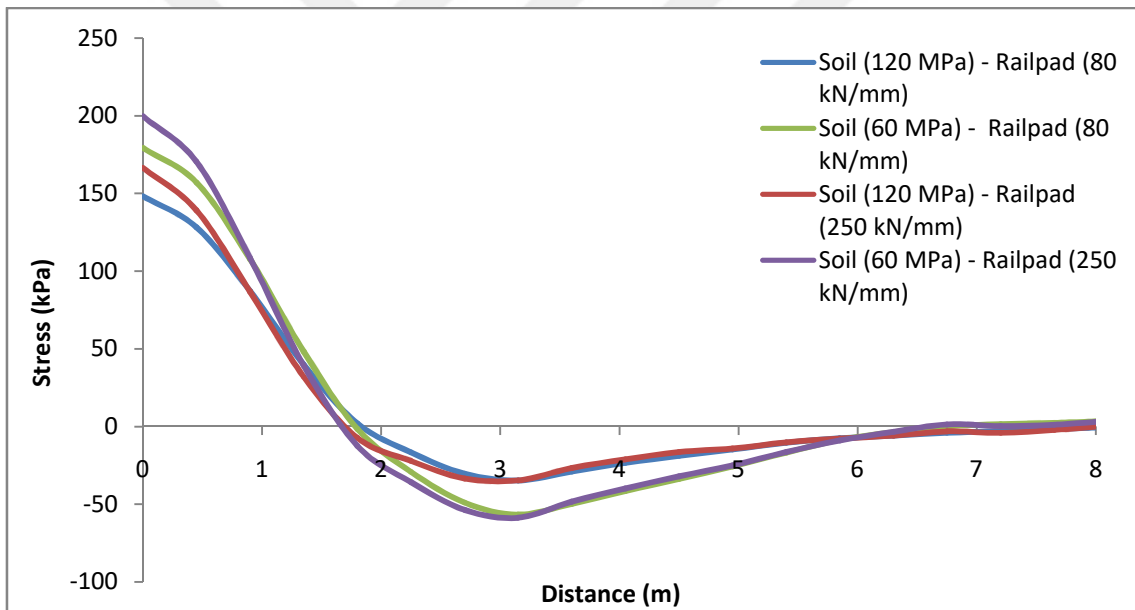


Figure 4-7 Horizontal stress results in the longitudinal direction for models produced using asphalt material in the lower slab layer

Model / Soil Stiffness	120 MPa		90 MPa		60 MPa	
	Transverse Stress (kPa)	Longitudinally Stress (kPa)	Transverse Stress (kPa)	Longitudinally Stress (kPa)	Transverse Stress (kPa)	Longitudinally Stress (kPa)
Design 1	91	177	96	197	103	275
Design 2	94	148	106	164	104	179
Design 3	99	199	104	221	110	300
Design 4	102	166	113	183	111	199

Table 4-5 Horizontal Stress for both direction for all models

4.3 Dynamic Results

In this section, dynamic effects which are a result of acceleration, displacement, vibration frequency and velocity under the track simulated by the method described in section 3.3 are presented.

4.3.1 Acceleration

Acceleration values are one of the crucial parameters that provide information about the dynamic behaviour of the structure under loads. The up and down movement of the slab causes too much resistance force, which is what is taken into account in the dynamic analysis. In this section, acceleration values calculated with the similar method described in section 3.3 are presented, and their graphs are shown. Figure 4-8 shows the behaviour of acceleration along the track at all layers for model 1 at train speed of 250 km/h. Table 4-6 shows the acceleration values of 4 different models for 250 km / h in all layers. Table 4-7 and Table 4-8 show the variation of maximum acceleration values calculated for different layers using model 1 and model 7 ABAQUS output between 100 km/h and 300 km/h, respectively. Acceleration values in the tables and figures indicate the points just below the layer of rail, CBL and HBL layers, while the acceleration values at the soil layer are for the points taken above it.

Based on the results, it can be accepted that the main parameters affecting acceleration magnitude are train speed and depth. Axle load may be an important parameter affecting the acceleration, but since the axle load was not changed in this study, no related data to it could be produced. The difference in acceleration magnitude is calculated to be approximately nine times greater in all layers for velocity between 100 km/h and 300 km/h, similar to Lamas-Lopez et al. (2017) 's study. Moreover, the acceleration value decreases approximately ten times when descending from the bottom of the rail level to the top of the foundation. It shows that as the depth increases, the dynamic effect decreases, as expected. Additionally, while it is one of the important parameters affecting the acceleration in the railpad, it has been observed that the change of soil stiffness does not affect the rail acceleration in parallel with Lei and Zhang (2011)'s work.

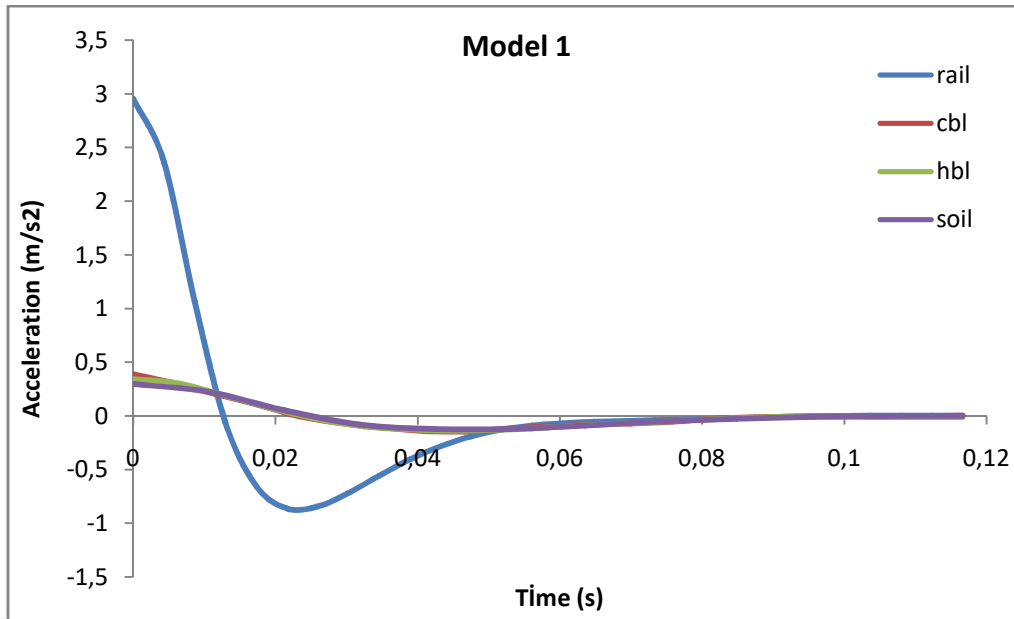


Figure 4-8 Change of acceleration throughout the track for all layers

Layer / Models	Model 1	Model 3	Model 4	Model 6
Rail	2,955408	3,094431	3,105683	3,22279
CBL	0,387155	0,524708	0,601343	0,73331
HBL	0,342793	0,478645	0,54416	0,672463
Soil	0,299277	0,431869	0,444748	0,557999

Table 4-6 Calculated maximum acceleration (m/s²) in all layers at train speed of 250 km/h for a different model

Layer / Train Speed	100 km/h	150 km/h	200 km/h	250 km/h	300 km/h
Rail	0,472865	1,063947	1,891461	2,955408	4,255787
CBL	0,154862	0,232293	0,309724	0,387155	0,464586
HBL	0,054847	0,123405	0,219387	0,342793	0,493621
Soil	0,047884	0,10774	0,191537	0,299277	0,430959

Table 4-7 Calculated maximum acceleration (m/s²) in all layers for different train speed (Model 1)

Layer / Train Speed	100 km/h	150 km/h	200 km/h	250 km/h	300 km/h
Rail	0,311853	0,701669	1,247411	1,949079	2,806674
CBL	0,180735	0,271103	0,36147	0,451838	0,542205
HBL	0,062094	0,139712	0,248377	0,388089	0,558848
Soil	0,053245	0,1198	0,212978	0,332779	0,479201

Table 4-8 Calculated maximum acceleration (m/s²) in all layers for different train speed (Model 7)

As can be seen from Table 4-7, it has been observed that the rise in the speed of the train significantly increases the acceleration value at the rail. While the acceleration value under the rail at train speed of 100 km/h is 0.47 m/s^2 , this value reaches as high as 4.25 m/s^2 for a train speed of 300 km/h. A descending from rail level, it is seen that the acceleration value decreases considerably at all train speeds. While the acceleration value calculated under the rail for 250 km/h is 2.95 m/s^2 , the acceleration value under the concrete slab layer is calculated as low as 0.38 m/s^2 . In fact, since the part that is in direct contact with the moving load is the rail, it is possible that the acceleration values on the rail are greater than the other layers, but the difference between the layers is massive. This severe drop in acceleration may have been caused by the railpad used under the rail. Considering that the use of a stiff rail pad also reduces the difference in acceleration between layers, it can be said that the rail pad used under the rail decrease the acceleration differences between layers.

When the data in Table 4-7 and the data in Table 4-8 are compared, it is seen that the acceleration values in the rail significantly decreases in the Model 7 using a stiff rail pad, while the acceleration values increases slightly in all other layers. Using a more stiff railpad may cause an increase in the centralized force to which the layers (for CBL, HBL and soil) are subjected. Since this extra force will force the layers to move more, it may have caused the acceleration values in the CBL, HBL and soil layers to tend to increase slightly. Table 4-6 shows the effect of soil stiffness on acceleration. Between model 1(120 Mpa soil stiffness) and model 3 (60 MPa soil stiffness) using concrete sub-slab in both, and between model 4 (120 Mpa soil stiffness) and model 6 (60 MPa soil stiffness) using asphalt slab in both, there is not much change in the rail acceleration values compared to the railpad effect calculated for 250 km/h train speed. While the difference in acceleration is around 4 - 5 percent for different soil stiffness, that of is more than 50 percent when changing railpad hardness.

Figure 4-9 and Figure 4-10 plots the change of acceleration values under the rail and CBL layer along the track for different models, respectively. The soil Young's modulus is 120 MPa in all models used in both comparisons.

From Figure 4-9, it can be seen how the materials used in slab tracks affect the dynamic behaviour. While a railpad with a stiffness of 80 kN/mm is used in both Model 1 and Model 4, the stiffness of the railpad in model 7 and model 10 is 250 kN/mm. In addition to this, while Model 1 and Model 7 are designed using concrete at the lower slab layer, this material is asphalt in Model 4 and Model 10. As seen in the graph, the difference in the material used at the lower slab layer do not change the maximum acceleration value in rail much, while the railpad stiffness decreases the maximum acceleration at a reasonable rate. Considering that asphalt material, which is cheaper and easier to make, gives very similar results with concrete in terms of dynamic results, the use of asphalt material in slab track designs can reduce the workload and reduce the initial investment costs without loss of quality. The difference between the maximum acceleration values for different models is similar to the behaviour in the maximum displacement graphs. It is seen that there is a strong relationship between the two charts as the acceleration values are produced using the displacement values, which is the ABAQUS output. Similar to Model 1 and Model 4, where there is high displacement, the maximum acceleration values are also high. The maximum displacement decreases significantly in the use of stiffer railpads, and the acceleration values are lower in models with more stiff railpads compared to models with less stiff railpads. However, when the effects of the use of different materials in the slab track design on the acceleration in the CBL layer is examined (Figure 4-10), the results are in the opposite direction of the effects on the rail. While the material used in the lower slab layer affected the acceleration change in the CBL layer more, the use of different rail pads do not cause much change in the acceleration. Furthermore, the use of more stiff railpads causes an increase in the acceleration value in the CBL layer, which is the opposite situation compared to rail.

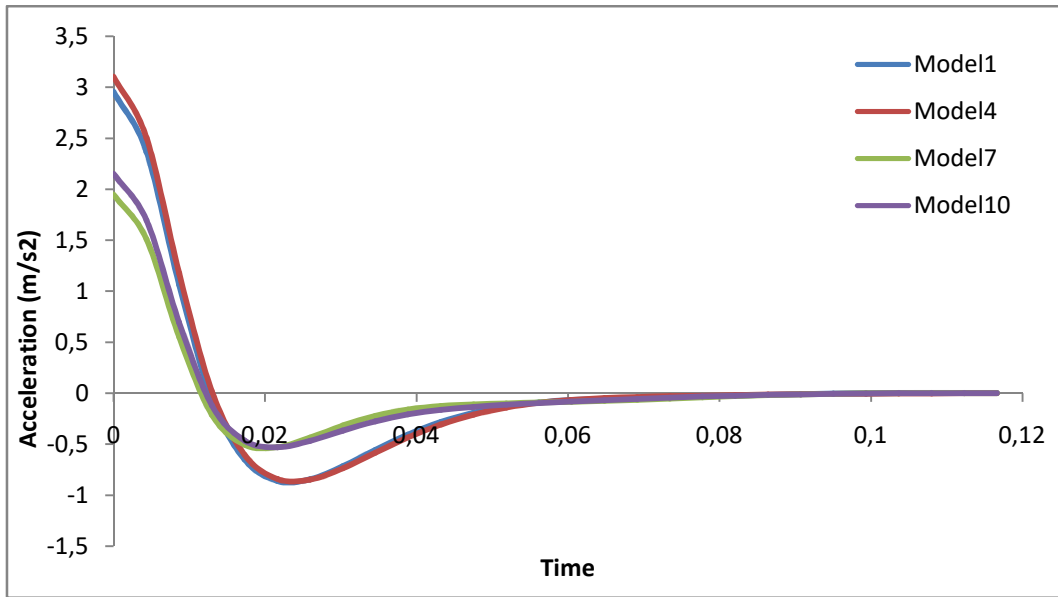


Figure 4-9 Comparison of rail acceleration along the track

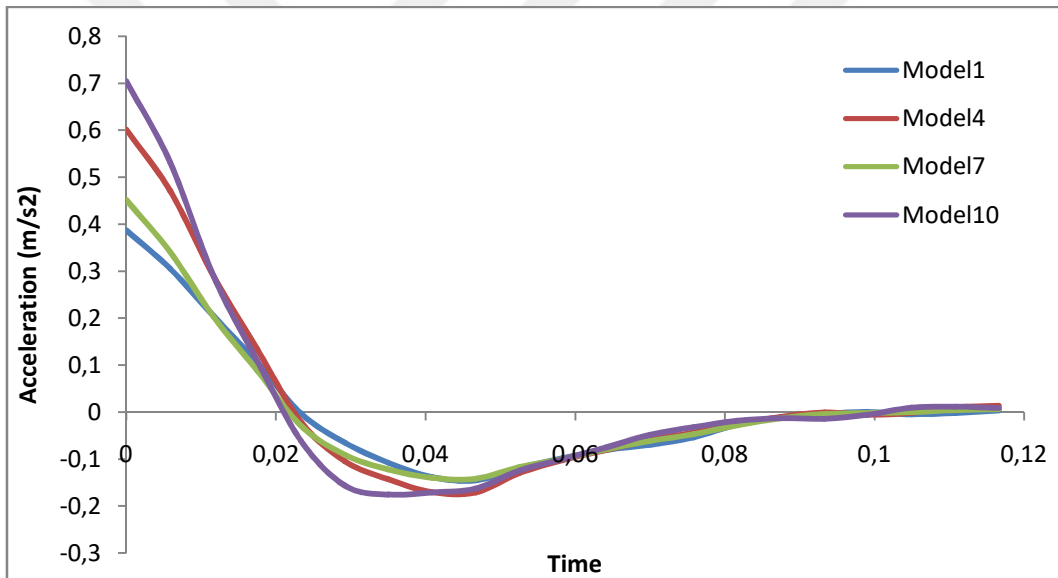


Figure 4-10 Comparison of CBL layer acceleration along the track

4.3.2 Displacement

Since the displacement behaviour of the track under loading is an important indicator, displacements on the concrete layer under the rail and top of the soil layer is analyzed for designs from models 1 to 6.

During dynamic loading, the extra stress led by the resistance of the layers against movement causes the displacements to be higher than with static analysis. In addition, vertical displacements are expected to increase with increasing train speed Kece, Reikalas et al. (2019), Yang, Gu et al. (2015), Nsabimana and Jung (2015) have proven that as the train speed increases, the displacement occurring on the track and soil increases. Along with this, the decrease in soil stiffness also causes the displacements observed to increase.

Displacements occurring at the top of the slab layer are not reasonable for a speed of 100 km / h. Any vertical displacement result could not be obtained for model 2 and model 4. In the meantime, displacement results of model 3 and model 6 were found to be 100% higher than that of static analysis which is quite above the expected rate of increase. The reason for not getting results at low speeds may be due to the increase in time interval with decreasing train speed. Since the displacement data is generated by integrating the velocity, higher dx interval between the two data may cause an error as a result of the integral. Another possibility is that vertical stress values gotten from ABAQUS outputs are not approximate results. The models that have more than expected increase in displacement (models 3 – model 6) have similar characteristics and the difference between the models is the material used in the lower slab. While concrete was used in models 3, asphalt is used in model 6. Failure to obtain results from similar models increases the probability of errors in the data used as input in the spreadsheet.

The change in maximum displacement at the slab layer and soil is shown in Figure 4-11 for the different model features described in section 4.1. The maximum displacement that occurred during the train passage and the displacement under the static weight of the train are also compared for different models in Figure 4-11. It can be seen that the maximum displacement obtained by performing dynamic analysis in all models is higher when compared with the results of static analysis which does not contradict the literature. Displacements

at slab and soil show different behaviours in dynamic analysis. Results of displacement at the top of soil have an increasing trend as train speed increases. However, this effect remained at a limited rate of around 4%. The reason for this may be that the dynamic effect decreases as go down from the rail level and the dynamic effect can be reflected more limitedly for the substructure in the calculation method. However, there is a reasonable increase in displacement for top of the slab layer, up to 15%, as the speed of train goes up. Here, it can be said that the dynamic effect is reflected partially better than the soil layer. The main difference in behaviour in terms of displacement at the slab layer and the soil occurs in models with softer soil stiffness. The maximum displacement at the soil layer tends to increase limitedly in softer soil (60 MPa) as train speed increases, which is 2.78 and 3.46 percent for model 3 and model 6, respectively. This is the opposite of the slab layer. Despite the increase in speed, displacement decreases and approaches static analysis results. When the train speed is 150 km / h, the vibration displacement of the slab is 0.419 and 0.421 m for models 3 and 6, respectively. However, as the speed goes up to 300 km / h, the displacement of the slab layer decreases by 0.4015 and 0.398 mm, which is very close to the static analysis results. In addition, the use of asphalt instead of concrete in the lower slab layer do not cause much change in the maximum displacement. Although concrete is a bit stiffer than asphalt, it is quite stiff in both materials. Due to the fact that the concrete spreads the exposed load slightly better than asphalt, relatively less displacement movements have been observed in the models using concrete in the lower slab layer.

Dynamic and static displacement results of from 1 to 6 models examined at different speeds are summarized in Table 4-9 for both layers.

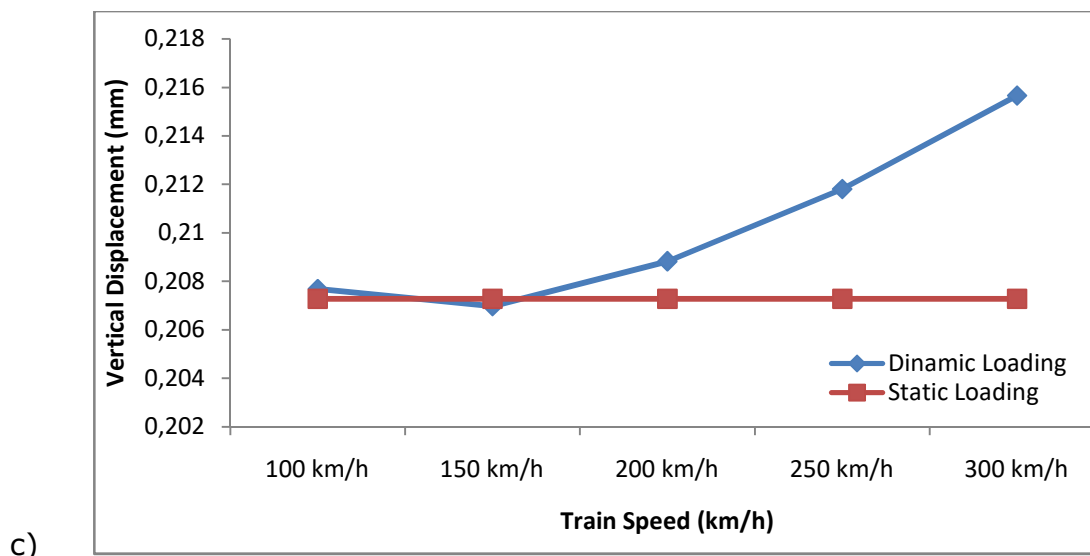
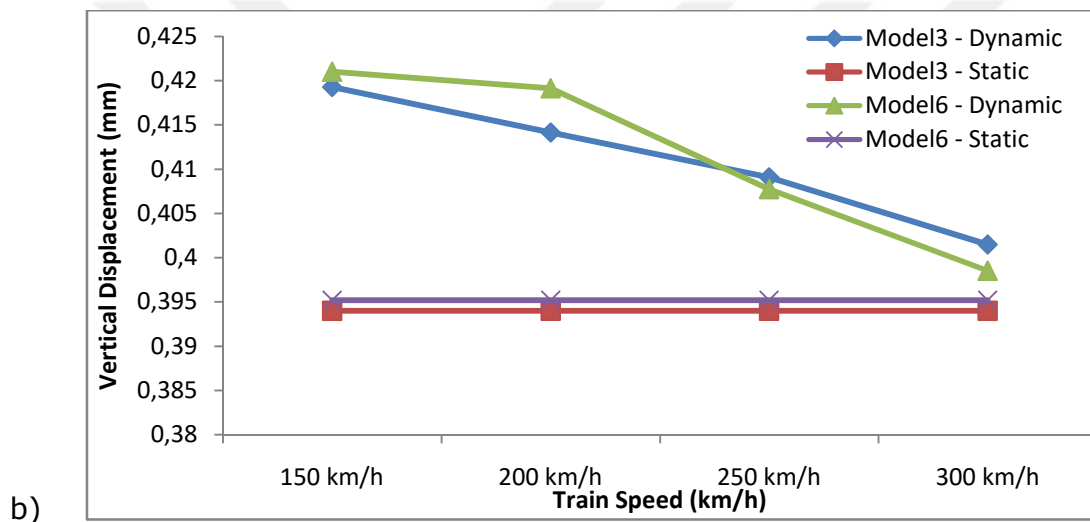
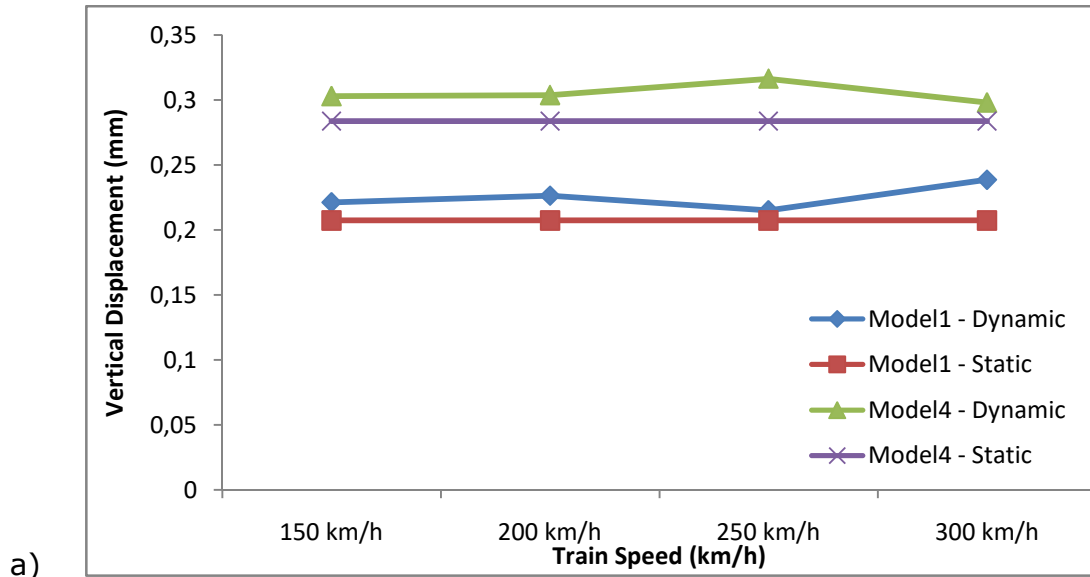


Figure 4-11 Maximum vertical displacement a)Slab layer for soil stiffness of 120 MPa b)Slab layer for soil stiffness of 60 MPa c)Soil layer for model 1

a)

Displacement (mm)						
Speed/Model	Model1	Model2	Model3	Model4	Model5	Model6
Static Loading	0,207296	0,243043	0,394018	0,283784	0,353332	0,3952
100 km/h	0,24422	error	0,79646	error	0,37999	0,78926
150 km/h	0,2213	0,25903	0,41928	0,30297	0,37724	0,421
200 km/h	0,22639	0,26704	0,41415	0,30385	0,36804	0,41913
250 km/h	0,21515	0,26219	0,40908	0,31646	0,37443	0,40776
300 km/h	0,23866	0,26842	0,4015	0,29809	0,3613	0,39854

b)

Displacement (mm)						
Speed/Model	Model1	Model2	Model3	Model4	Model5	Model6
Static	0,207276	0,243423	0,39455	0,28103	0,351188	0,392875
100 km/h	0,20769	0,24333	0,39325	0,281141	0,35077	0,391124
150 km/h	0,20698	0,24341	0,39513	0,28066	0,35115	0,39347
200 km/h	0,20883	0,24573	0,39892	0,28355	0,35506	0,39816
250 km/h	0,21181	0,24958	0,402	0,28843	0,36051	0,40278
300 km/h	0,21566	0,25298	0,4055	0,29304	0,3654	0,40646

Table 4-9 Maximum vertical displacement result for all model a)Slab layer b)Soil

4.3.3 Vibration properties

Vibrations behaviour occurring at slab and soil under moving load were examined for different train speeds and track models. The waves will tend to propagate differently along the track, along the slab, and along the ground so that these will have a different natural frequency. In this section, the different behaviours of vibrations occurring in slab and ground are examined. Since the time interval selected in the tool developed in Excel is not small enough for the vibration frequency on the rail, no result has been produced for the rail level. Figure 4-12 shows the plot of the wave velocity changes occurring at slab and soil with increasing moving load. Table 4-10 and Table 4-11 summarize the calculated wave frequency and velocity with the tools described in section 3.3 at the slab and soil layer, respectively.

As seen in Figure 4-12, it can be said that the model is mostly valid on soils with higher stiffness and at moving load up to 250 km/h. As expected, increasing train speed raises the number of vibrations occurring on the layer, and the frequency of the wave is expected to increase as the train speed increases. While

this situation can be clearly seen for model1, model2 and model4, the soil stiffness used in these models are 120, 90 and 120 MPa, respectively, models with lower stiffness moduli, which are Model 3 and Model 6, the expected increase in the speed of wave has been limited and a decrease in the velocity of the wave has been observed after 250 km/h speed of train.

It is expected that the number of vibrations during the passage of the train will be less in models with low soil modulus. Since a small area of 8 meters is examined in the developed model, it may have caused the calculated frequency and wave velocity values to be erroneous due to the low number of waves measured in these models. A similar situation has been observed in the investigations on the ground. The approximate method used in calculating the wave velocity on the soil surface did not give very accurate results. Since a length of 8 m was passed in 0.096 seconds for a train travelling at 300 km / h, only a single peak was formed in the displacement graph during this short time, and the vibration frequency and velocity at speeds could not be calculated.

The effect of using asphalt in the lower slab layer on the vibration characteristics was also investigated. Due to the more flexible behaviour of the asphalt layer compared to concrete, the number of vibrations on the track using asphalt is expected to be lower than the track using concrete. Although the viscous effect was ignored in the designed model, vibration frequency and speed were found to be lower in models using asphalt compared to the concrete layer. When the models 1- 4 and model 2 - 5, which have precisely the same properties except for the material used in the lower slab, are compared, the frequency of the vibration induced by the train at 250 km/h is 20% and 38% lower in the model using asphalt sub-slab. While the velocity of the wave in model 1 and model 2 is 341 m/s and 303 m/s, respectively, these values are 299 m/s and 246 m/s in models 3 and 4, respectively. It shows that the use of asphalt slab may give better results than using concrete at the lower slab for the degradation caused by vibration to which the soil is exposed.

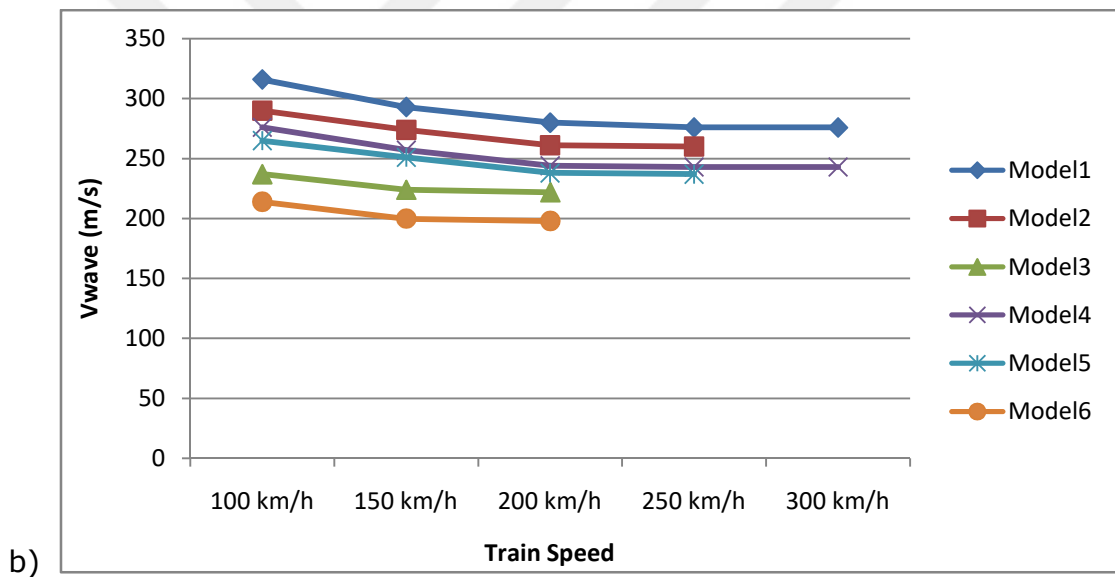
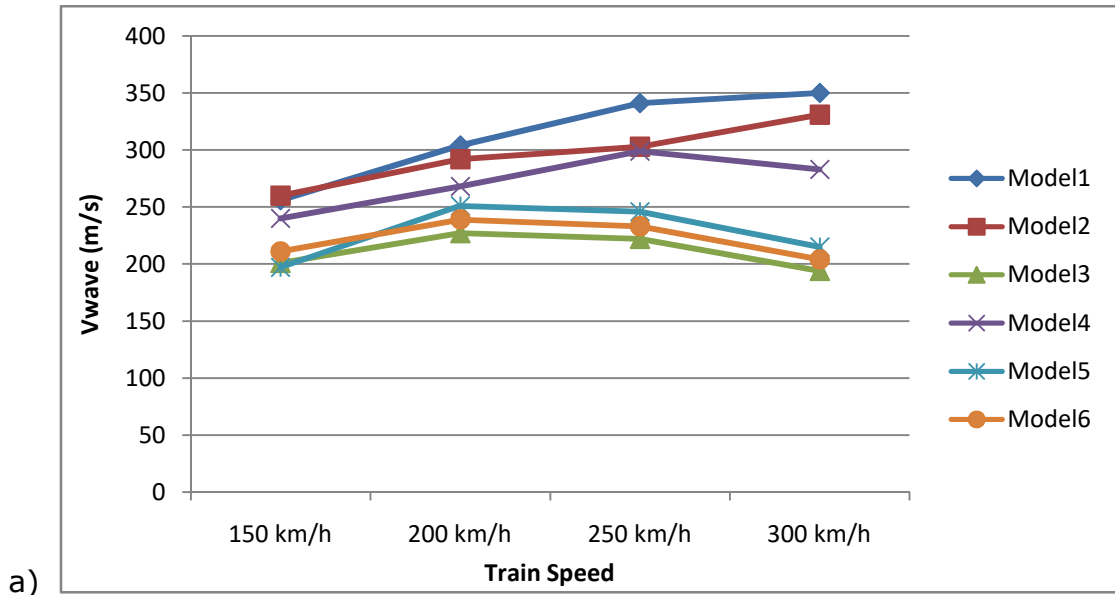


Figure 4-12 Comparison of the wave velocities plotted against the different train speed a)for slab layer b) for top of the soil

a)

Slab Layer	Frequency (Hz)					
Speed/Model	Model1	Model2	Model3	Model4	Model5	Model6
100 km/h	111	92	51	92	62	54,7
150 km/h	62	63,5	51	56,8	46	50,86
200 km/h	73	71,3	57,6	63,5	59	57,45
250 km/h	82	74,1	56,4	70	58	56
300 km/h	84	81,02	49,3	67	50	49

b)

Soil	Frequency (Hz)					
Speed/Model	Model1	Model2	Model3	Model4	Model5	Model6
100 km/h	28	24,97	18,34	27,68	23,99	18,99
150 km/h	26,7	23,57	17,33	25,83	22,72	17,74
200 km/h	25,5	22,43	17,22	24,57	21,57	17,54
250 km/h	25,2	22,36	-	24,46	21,51	-
300 km/h	25,2	-	-	24,4	-	-

Table 4-10 Calculated wave frequencies in examined models for different train speed a) for slab layer b) for a top of the soil

a)

Slab Layer	Vwave (m/s)					
Speed/Model	Model1	Model2	Model3	Model4	Model5	Model6
100 km/h	458	379	201	391	264	228
150 km/h	256	260	201	240	197	211
200 km/h	304	292	227	268	251	239
250 km/h	341	303	222	299	246	233
300 km/h	350	331	194	283	215	204

b)

Soil	Vwave (m/s)					
Speed/Model	Model1	Model2	Model3	Model4	Model5	Model6
100 km/h	316	290	237	276	265	214
150 km/h	293	274	224	257	251	200
200 km/h	280	261	222	244	238	198
250 km/h	276	260	-	243	237	-
300 km/h	276	-	-	243	-	-

Table 4-11 Calculated wave velocities in examined models for different train speed a) for slab layer b) for a top of the soil

5 Discussion and Conclusion

5.1 Discussion

In this section, estimation of the dynamic behaviour of slab track structures can be made approximately with data derived from static analysis results. Based on this, a 3D model was first developed in ABAQUS, finite element software, to learn the behaviours that occur under static load. Later, an approach was derived from a tool developed in Excel to interpret the dynamic effects occurring under the slab track. In this section, assumed approaches in developed 3D model, methods used and comparison of analysis results will be discussed by looking at the literature.

The first point of the study is to develop a model that realistically represents the slab track behaviour in the loading state. Many different programs have been used for this, such as ABAQUS, Ansys, Plaxis, Nastran. The program preferred in this study is the ABAQUS software used by many people, such as Nsabimana and Jung (2015) and Matias and Ferreira (2020). Important parameters to be considered while modelling in this program can be listed as to how the connection between layers is made, boundary conditions and mesh size. In this thesis, the type of constraint used between layers is the same with Shih (2017) and Connolly (2013). Mesh sizes were determined by taking into account the element positions as in Arañó Barenys (2016) 's study, but there was a limitation in the use of nodes (1000 nodes) due to the student version of the ABAQUS software used. For this reason, the mesh sizes could not be adjusted correctly. The negative effect of this situation is seen in the vertical stress graphs described in section 4.2.2 at the CBL layers.

Another critical point is the realistic representation of the wheel-rail interaction. Due to the limited time and long calculation time of dynamic analysis, this interaction was ignored, and only static loading was performed in this study and dynamic data was produced with the developed tools. After finding the acceleration value with the calculation described in Section 4.3.1, the displacements under dynamic conditions are calculated by taking the integral of the acceleration value twice, similar to the method used in Lamas-Lopez et al. (2017)'s work. Similarly, the acceleration results calculated for different

velocities were obtained by taking the two times differential of the displacement data under static loads, which is the output of ABAQUS.

One of the other crucial stages of the study is that the displacement and stress values obtained as a result of the static analysis are approximate results that do not contradict with the literature. Because if these results are wrong, it means that the dynamic data obtained by using static analysis results, which is the second step of the study, are wrong. Also, differences in slab behaviour as a result of the changes in the materials used in the layers (such as a change in ground stiffness, using a more rigid rail pad) should not contradict the literature.

At this stage, the maximum vertical displacement results from the ABAQUS outputs of Model 1 designed with the materials generally used in slab track design are quite similar to the research results of He et al. (2018), Kece et al. (2019a), Yang et al. (2015), Nsabimana and Jung (2015). The vertical soil pressure results in the models called ST1 and ST5 in Prakoso (2017) 's study are quite compatible with the values in this thesis.

The maximum displacement values in the rail in He et al. (2018) and Kece et al. (2019b) 's study, and the maximum displacement values in the soil in Nsabimana and Jung (2015)'s study was around 0.6 mm and 0.4 mm, respectively, which is entirely consistent with the findings in this thesis. Furthermore, the vertical stress values of 11.92 MPa and 9.39 MPa on the soil in the models called ST1 and ST2 developed by Prakoso (2017), respectively, are close results with models 3 and model 6, which are quite similar designs.

As a result of the analysis, it was found that the longitudinal tensile stresses (S33) in the HBL layer are higher than the transverse tensile stresses (S22), the vertical stress and longitudinal tensile stresses are dominant in the HBL layer, which does not contradict the study done by Liu et al. (2019). Additionally, when the models with lower soil moduli ($E = 60$ MPa) are compared with the models with stiffer soils ($E = 120$ MPa); It has been found that while vertical displacement decreases, longitudinal tensile stresses increase and larger displacements occur, which is in parallel with Liu et al. (2019), Nsabimana and Jung (2015) and Prakoso (2017)'s study.

Regarding the effect of the parameters changed in the model on the displacement, Shih (2017), Nsabimana and Jung (2015), Yang et al. (2015), Lei and Zhang (2011) found that the increase in the train speed raised the displacement. Moreover, Yang et al. (2015) investigated the effect of change in train speed on acceleration and found that the acceleration observed in the layers increases as the speed increases in parallel with the displacement. As can be seen from Table 4-7, the effect of speed change on acceleration is entirely parallel with the literature, but the results of the acceleration show a limited similarity in the literature. The displacement graph (Figure 4-11) plotted against the train speed for the soil layer is very similar to Nsabimana and Jung (2015)'s study that the displacement increases as the speed increases. However, similar results were not obtained for the slab layer; the increase in displacement was achieved for values between 150 km/h and 250 km/h. No meaningful data could be produced for the speed of lower than 150 km/h and greater than 250 km/h.

One of the other examined materials is railpad. As expected, the use of a harder railpad significantly reduces the vertical displacement and the acceleration of the rail, while the slab acceleration has been found to increase slightly, which is similar to Lei and Zhang (2011)'s work. Although the acceleration values in the rail calculated in the tool developed in Excel do not give an approximate result with the literature, the results are more approximate as the rail level is descended. In particular, the acceleration results calculated by He et al. (2018) on the concrete surface correspond to the data found in this thesis. Also, the graph showing the behaviour along the track of the acceleration on the slab caused by the freight trains found by He et al. (2018) is very similar to the result of this study, due to the fact that the slow movement of freight trains is similar to the static loading.

5.2 Conclusion

In this thesis, finite element models have been created to examine the dynamic and static response occurring in the substructure and superstructure in slab track structures by using software ABAQUS and Excel. Static analysis data were produced with the software ABAQUS, and then a dynamic interpretation was made with the tools developed in Excel with ABAQUS outputs. With the different models developed, the effects of different materials on displacement, acceleration and stress were evaluated according to both static analysis and dynamic analysis results. According to the analysis results, the findings can be summarized as follows.

Static Analysis;

- While the most critical parameters affecting the displacement on the rail are the railpad stiffness and soil modulus, it has been observed that the material difference used in the lower slab layer (concrete or asphalt) does not change the rail displacement very much, especially in models with low soil modulus and models used concrete sub-slab. This situation is slightly different from the rail in the CBL layer. While the effect of the soil module on the displacement in the CBL is similar to the rail, the change in the railpad stiffness caused the opposite of the effect seen on the rail and the displacement values in CBL layer increased with the use of a stiffer railpad. Further, the difference of material used in the sub-slab layer does not affect the displacement in the rail whereas the use of asphalt material in the CBL layer with the high young's modulus soils increases the displacement considerably.
- Regarding the stress results, dominant stresses are longitudinal horizontal stress and vertical stress. While vertical stress value is high in stiff soils, longitudinal stress is higher in lower Young's modules soils. Moreover, The change in the stiffness of the railpad does not affect the vertical and longitudinal stress much, the type of material used in the lower slab and the change in the soil stiffness has the converse effect on vertical stress and longitudinal stress. Although the use of asphalt sub-slab significantly reduces the longitudinal stress compared to using concrete sub-slab, especially in soils with low Young's modulus, it causes an increase in vertical stress with the use of stiff soils.

Dynamic Analysis;

- The further away from the rail level, the dynamic effects decline and the findings obtained as a result of dynamic analysis and the results of static analysis are quite similar to each other.
- The increase in train speed results in an increase in the acceleration value in all layers, which indicates that the track is under more dynamic effects. By comparing different models developed using different material properties, it was found that the most remarkable parameters that will reduce this increased dynamic effect are the railpad for the rail and the stiff soil for the CBL layer. Besides, train speed has been found to be a significant parameter affecting displacement.
- For the vibration, vibration frequency and velocity in each layer are different from each other, and the soil elasticity module and the type of material used in the lower slab layer are the factors that significantly affect the vibration characteristics.

When all the findings are evaluated, a mixed model can be developed by using concrete and asphalt materials together in the slab track design and mixed slab track design can be considered as a solution to the problems encountered in slab track designs such as vibration problem, excessive initial investment cost and excess labour required during construction.

5.3 Future Research

Some studies in this thesis can be extended, the first of which is the model designed in Abaqus for getting static analysis result. More realistic results can be obtained by removing the limitations in section 1.2 and including the assumptions mentioned in Section 3.1 into the model. The second may develop more advanced tools than this thesis, which convert static data into dynamic results. Thus, an alternative method to techniques that are very expensive in terms of both time and resources can be proposed, which is realized by Bezgin and Kolukirik (2019) by proposing analytical equations to estimate the dynamic impact forces created by the wheel flats on the railway.

6 References

- ARAÑÓ BARENYS, A. 2016. *Evaluation of 3D Dynamic Effects Induced by High-speed Trains on Double-track Slab Bridges*. Universitat Politècnica de Catalunya.
- AUERSCH, L. 2006. Dynamic axle loads on tracks with and without ballast mats: numerical results of three-dimensional vehicle-track-soil models. *Proceedings of the Institution of Mechanical Engineers, Part F: Journal of Rail and Rapid Transit*, 220, 169-183.
- BEZGIN, N. & KOLUKIRIK, C. 2019. *Development Of The Bezgin-Kolukirik Equation To Estimate Dynamic Impact Forces Generated By Wheel Flats On Railway Tracks*.
- BIAN, X.-C., CHAO, C., JIN, W.-F. & CHEN, Y.-M. 2011. A 2.5 D finite element approach for predicting ground vibrations generated by vertical track irregularities. *Journal of Zhejiang University-Science A*, 12, 885-894.
- BIAN, X., JIANG, H., CHENG, C., CHEN, Y., CHEN, R. & JIANG, J. 2014. Full-scale model testing on a ballastless high-speed railway under simulated train moving loads. *Soil Dynamics and Earthquake Engineering*, 66, 368-384.
- CHO, Y. K., KIM, S.-M., CHUNG, W., KIM, J. C. & OH, H. J. 2014. Effect of steel ratio on behavior of Continuously Reinforced Concrete Railway Track under environmental loads. *KSCE Journal of Civil Engineering*, 18, 1688-1695.
- CONNOLLY, D. 2013. Ground borne vibrations from high speed trains.
- CONNOLLY, D. P., KOUROUSSIS, G., LAGHROUCHE, O., HO, C. & FORDE, M. 2015. Benchmarking railway vibrations–Track, vehicle, ground and building effects. *Construction and Building Materials*, 92, 64-81.
- COOPER, J. H. & HARRISON, M. F. Development of an alternative design for the West Rail viaducts. *Proceedings of the Institution of Civil Engineers-Transport*, 2002. Thomas Telford Ltd, 87-95.
- DUAN, X., HU, J., BIAN, X. & JIANG, J. Dynamic interaction of vehicle-track coupled system under different patterns of uneven settlement. *International Symposium on Environmental Vibration and Transportation Geodynamics*, 2016. Springer, 565-573.
- ESVELD, C. 2001. *Modern railway track*, MRT-productions Zaltbommel, Netherlands.

- FREUDENSTEIN, S. 2010. RHEDA 2000®: ballastless track systems for high-speed rail applications. *International Journal of Pavement Engineering*, 11, 293-300.
- FRÝBA, L., NAKAGIRI, S. & YOSHIKAWA, N. 1993. Stochastic finite elements for a beam on a random foundation with uncertain damping under a moving force. *Journal of sound and vibration*, 163, 31-45.
- GALVÍN, P., ROMERO, A. & DOMÍNGUEZ, J. 2010. Fully three-dimensional analysis of high-speed train-track-soil-structure dynamic interaction. *Journal of Sound and Vibration*, 329, 5147-5163.
- HE, Q., CAI, C., ZHU, S., ZHANG, J. & ZHAI, W. 2018. Dynamic performance of low vibration slab track on shared high-speed passenger and freight railway. *Transport*, 33, 669-678.
- KECE, E., REIKALAS, V., DEBOLD, R., HO, C. L., ROBERTSON, I. & FORDE, M. C. 2019a. Evaluating ground vibrations induced by high-speed trains. *Transportation Geotechnics*, 20.
- KECE, E., REIKALAS, V., DEBOLD, R., HO, C. L., ROBERTSON, I. & FORDE, M. C. 2019b. Evaluating ground vibrations induced by high-speed trains. *Transportation Geotechnics*, 20, 100236.
- KUO, C.-M., HUANG, C.-H. & CHEN, Y.-Y. 2008. Vibration characteristics of floating slab track. *Journal of Sound and Vibration*, 317, 1017-1034.
- LAMAS-LOPEZ, F., CUI, Y.-J., CALON, N., D'AGUIAR, S. C. & ZHANG, T. 2017. Impact of train speed on the mechanical behaviours of track-bed materials. *Journal of Rock Mechanics and Geotechnical Engineering*, 9, 818-829.
- LEI, X. 2016. *High speed railway track dynamics: Models, algorithms and applications*, Springer.
- LEI, X. 2017. *High speed railway track dynamics*, Springer.
- LEI, X., WU, S. & ZHANG, B. 2016. Dynamic analysis of the high speed train and slab track nonlinear coupling system with the cross iteration algorithm. *Journal of Nonlinear Dynamics*, 2016.
- LEI, X. & ZHANG, B. 2011. Analysis of Dynamic Behavior for Slab Track of High-Speed Railway Based on Vehicle and Track Elements. *Journal of Transportation Engineering*, 137, 227-240.

- LIU, S., CHEN, X., MA, Y., YANG, J., CAI, D. & YANG, G. 2019. Modelling and in-situ measurement of dynamic behavior of asphalt supporting layer in slab track system. *Construction and Building Materials*, 228, 116776.
- LIU, X., ZHAO, P. & DAI, F. 2011. Advances in design theories of high-speed railway ballastless tracks. *Journal of Modern Transportation*, 19, 154-162.
- MATIAS, S. R. & FERREIRA, P. A. 2020. Railway slab track systems: review and research potentials. *Structure and Infrastructure Engineering*, 1-19.
- MICHAS, G. 2012. Slab track systems for high-speed railways.
- NSABIMANA, E. & JUNG, Y.-H. 2015. Dynamic subsoil responses of a stiff concrete slab track subjected to various train speeds: a critical velocity perspective. *Computers and Geotechnics*, 69, 7-21.
- PRAKOSO, P. B. 2017. *Analysis and Evaluation of Railway Track Systems on Soft Soil: Trackbed Thickness Design and Dynamic Track-Soil Interaction*. Technische Universität München.
- REN, J., LI, X., YANG, R., WANG, P. & XIE, P. 2016. Criteria for repairing damages of CA mortar for prefabricated framework-type slab track. *Construction and Building Materials*, 110, 300-311.
- SHIH, J.-Y. 2017. *Models for vehicle/track/ground interaction in the time domain*. University of Southampton.
- SHIH, J.-Y., KOSTOVASILIS, D., BEZIN, Y. & THOMPSON, D. 2017. *Modelling options for ballast track dynamics*.
- SONG, X., ZHAO, C. & ZHU, X. 2014. Temperature-induced deformation of CRTS II slab track and its effect on track dynamical properties. *Science China Technological Sciences*, 57, 1917-1924.
- SSF INGENIEURE 2010. Slab track systems on different substructures. *Company brochure*.
- STEENBERGEN, M., METRIKINE, A. & ESVELD, C. 2007. Assessment of design parameters of a slab track railway system from a dynamic viewpoint. *Journal of Sound and Vibration*, 306, 361-371.
- THOMPSON, D. & GAUTIER, P. 2006. Review of research into wheel/rail rolling noise reduction. *Proceedings of the Institution of Mechanical Engineers, Part F: Journal of Rail and Rapid Transit*, 220, 385-408.
- WANG, M., CAI, C., ZHU, S. & ZHAI, W. 2017. Experimental study on dynamic performance of typical nonballasted track systems using a full-scale test

- rig. *Proceedings of the Institution of Mechanical Engineers, Part F: Journal of Rail and Rapid Transit*, 231, 470-481.
- WARBURTON, G. B. 1976. *The dynamic behavior of structures, 2nd Edition*, Oxford, Pergamon Press.
- YANG, X., GU, S., ZHOU, S., YANG, J., ZHOU, Y. & LIAN, S. 2015. Effect of track irregularity on the dynamic response of a slab track under a high-speed train based on the composite track element method. *Applied Acoustics*, 99, 72-84.
- ZHANG, X., BURROW, M. & ZHOU, S. 2016. An investigation of subgrade differential settlement on the dynamic response of the vehicle-track system. *Proceedings of the Institution of Mechanical Engineers, Part F: Journal of Rail and Rapid Transit*, 230, 1760-1773.
- ZHU, S. & CAI, C. 2011. Fatigue life prediction of CRTS I ballastless slab track. *ICTE 2011*.
- ZHU, S. & CAI, C. 2014. Interface damage and its effect on vibrations of slab track under temperature and vehicle dynamic loads. *International Journal of Non-Linear Mechanics*, 58, 222-232.
- ZHU, S., FU, Q., CAI, C. & SPANOS, P. D. 2014. Damage evolution and dynamic response of cement asphalt mortar layer of slab track under vehicle dynamic load. *Science China Technological Sciences*, 57, 1883-1894.

